Spatial distribution of bed level changes and responsible sediment exchanges across the Dutch shoreface

---

Master thesis project

Kamiel Röell
23 September 2022

Utrecht University
Faculty of Geosciences
Department of Physical Geography

Deltares
Zee en Kust Systemen
Applied Morphodynamics

Supervisors:
J.H. Nienhuis
B.T. Grasmeijer

Universiteit Utrecht

Deltares
Enabling Delta Life

Abstract

The lower shoreface is an important part of the coast because it is the foundation of the beach and dunes that prevent the hinterland from flooding. The lower shoreface has been under reviewed and sediment transport and the morphodynamics have been poorly quantified. The study objectives are therefore to quantify the large-scale bed level changes, find the responsible sediment exchanges and validate the transport model results of Grasmeijer et al. (2022). Bathymetric changes based on Vaklodingen between 2019-2017 and transport data between 2013-2017 from Grasmeijer et al. (2022) are combined to study the shoreface of the Dutch Holland coast in different zones (both longshore and depth-dependant cross-shore). The results show flattening of the lower shoreface due to larger net erosion in the shallow part compared to the deeper part. Three sections were identified: an eroding northern section, an accumulating central section and a stable southern section. The modelled transport data shows an increasing total and longshore transport towards the north due to increasing tidal flood dominance (Grasmeijer et al., 2022). The overall onshore-directed cross-shore transport increased towards smaller water depths. The modelled transports were shown to result in longshore and cross-shore exchanges. These are dependent on the transport magnitude, the shoreface width and the vicinity of mega nourishment. The shoreface width modulates the length of the lateral boundaries and seaward boundary is curving so that transport is oblique to this boundary along the majority of the shoreface This results in alongshore sediment exchanges for the different zones. Additionally, bathymetry- and transport-based sediment volume changes are determined and compared. The volumes show almost no resemblance. Possible explanations are inaccuracies of the bathymetric data, the excluded sediment exchange with the upper shoreface and the excluded effect of undertow in the transport model results. Vaklodingen result seem to result in uncertainties so the results must be considered carefully. The combination of bathymetric data and modelled transport data however is a useful method to study the lower shoreface.

Content

1. Introduction

1.1 Background information and problem formulation

The shoreface is the sloping transition zone between the coastline and the continental shelf. The shoreface forms the foundation of the subaerial dunes and beach that function as natural barriers to safeguard the hinterland from flooding hazards (e.g. Quataert et al., 2021). It is therefore necessary maintain the coastal foundation. With that, an artificial supply of sand is required to the coastal zone to counteract coastal recession and prevent flooding because of the rising sea levels (Rijkswaterstaat, 2020; van der Werf et al., 2017). In the Netherlands, it is coastal management policy since 1990 is to supply sand to the coastal foundation (see Figure 1) using shoreface nourishments to make sure that the coast is in an dynamic equilibrium. This strategy of shoreface nourishments depends on natural processes to transport and distribute the sand from the nourished area to the regions where it is needed the most (e.g. Brand et al., 2022). However, to effectively apply shoreface nourishments to maintain the coastal foundation, it is necessary to understand the bed-level evolution of the shoreface (Hinton & Nicholls, 2007) and the processes that are responsible (e.g. Grasmeijer et al., 2022; Spek et al., 2020; Vermaas et al., 2015).

The hydrological and morphological processes across the shoreface are driven by a dynamic mixture of waves, tides and currents. Because of the large extent of the shoreface and the seaward decaying water depth, processes are spatially variable. As a result, the shoreface can be split up in the shallow upper and deeper lower shoreface. The upper shoreface is prone to wave processes such as breaking, dissipation, return and longshore currents. The upper shoreface is active and responds morphodynamically on short timescales (i.e. days to years). The lower shoreface is generally driven by shoaling waves and tidal processes and is much less active and responds on much larger timescales (i.e. years to decades) (e.g. Ortiz & Ashton, 2016; Vermaas et al., 2015). Sediment transport processes and morphodynamics on the upper shoreface have received much more attention compared to the lower shoreface as a result (Anthony & Aagaard, 2020). Small morphodynamic changes over large surface areas such as the lower shoreface result in the exchange of large sediment volumes (Anthony & Aagaard, 2020). Therefore, the lower shoreface requires more focus.

Nevertheless, progression has been made over the past decades to better understand the lower shoreface. The lower shoreface has received increasing interest with regard to sediment shortage due coastal recession and the sea level rise (Aagaard, 2011, 2014; Backstrom et al., 2009; Grasmeijer et al., 2022; Kleinhans & Grasmeijer, 2006; Ortiz & Ashton, 2016; Patterson & Nielsen, 2016; Spadon, 2000; Vermaas et al., 2015; Walburg, 2005). This occurred

especially in the Netherlands since the new coastal policy in 1990. However, it remains difficult to scale up transport processes towards lower shoreface scales using models (Anthony & Aagaard, 2020). Transport processes are sometimes not included in models which causes uncertainty (e.g. Knook, 2013). The recent study of Grasmeijer et al. (2022) presents a useful transport model for the Dutch shoreface, however the results of the model have not been validated morphodynamically. Moreover, field measurements on the lower shoreface are lacking (Anthony & Aagaard, 2020) and consequently models are difficult to calibrate and validate. Bathymetric data often does not cover the entire depth range of the lower shoreface (Van Rijn, 1997; Walburg, 2005) and responsible transport processes cannot be derived from bathymetry only (Spadon, 2000; Vermaas et al., 2015).

Combining bathymetric data and a transport model is potentially a powerful method to increase our understanding of the lower shoreface in terms of sediment exchanges and morphodynamics. Hence, van Rijn (1997) set up a sediment budget model for the Holland coast with such an approach. However, they could only validate the budget model for the zone landward of -12 m water depth by hindcasting the morphodynamic change because of the limited bathymetric data. The bathymetric data is least covering the shoreface for the Holland coast (Walburg, 2005). Consequently, the zone of the lower shoreface between -12 and -20 m was not validated properly. The knowledge on bed level (or volumetric) changes on the Dutch lower shoreface and the responsible sediment exchanges is therefore incomplete and should be expanded. The problem is addressed with this study through a combination of recent bathymetric data and the newly set-up transport model by Grasmeijer et al. (2022).

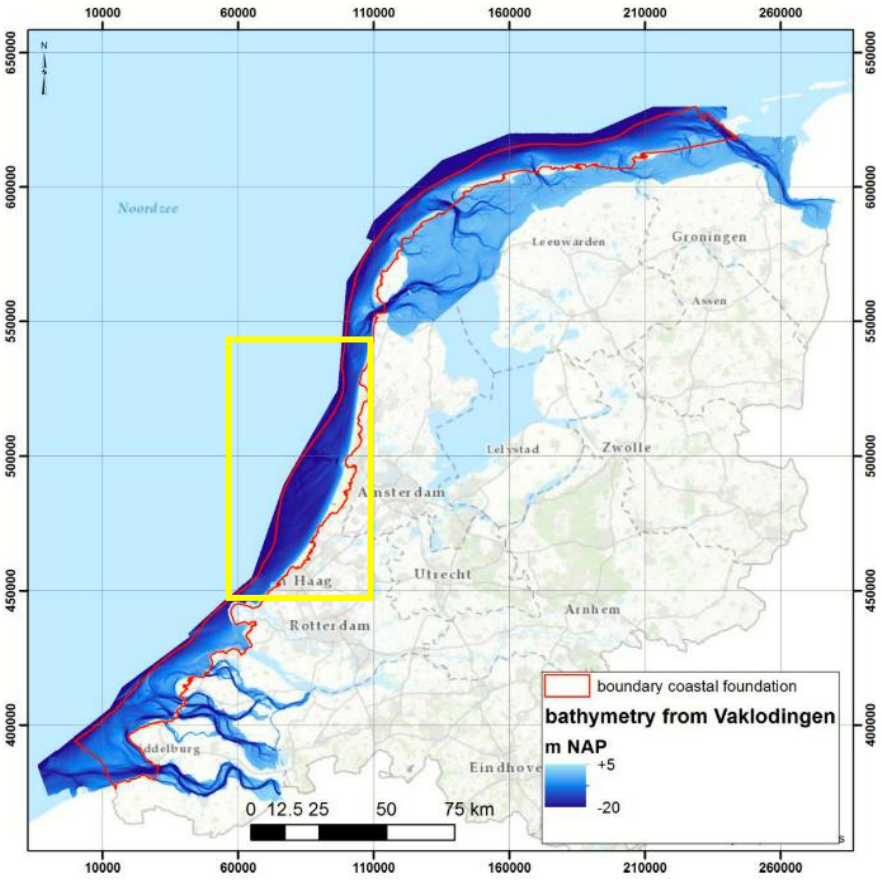

Figure 1: The Dutch shoreface and the study area (yellow box).

1.2 Objectives and approach

The research question is:

1. How did the largescale bathymetry on the Dutch lower shoreface evolve over the last decade and what are the responsible sediment exchanges on the Dutch lower shoreface?

The objectives for this study are as follows:

1. Quantification of the recent large-scale bed level changes across the lower shoreface of the Dutch Holland barrier coast to determine the spatial distribution.
2. Determination of the dominant sediment exchanges that are responsible for these large-scale bed level changes.
3. Morphodynamical validation of the lower shoreface transport model from Grasmeijer et al. (2022) for the Dutch Holland barrier coast.

Bathymetric data between 2008 and 2017 are used based on Vaklodingen to study the bed large-scale level changes in a number of subdivided zones of the lower shoreface. These results are combined with modelled shoreface sediment transport rates between 2013-2017

from Grasmeijer (2018) and Grasmeijer et al. (2022) to determine the sediment exchanges. The analyses are used to determine the recent (past decade) evolution of the lower shoreface in terms of bed level changes and the responsible sediment exchanges. To achieve the thrid goal, sediment volume changes based on both the measured bathymetry and on the modelled sediment transport are determined and compared.

1.3 Reading guide

The water depth in this study is given as m NAP which is the depth with respect to the Dutch datum for the mean sea level. Chapter 2 provides a literature review about shoreface transport mechanisms and the Dutch shoreface hydrodynamics, sediment transport and morphodynamics. Chapter 3 is a description of the methods used to achieve the objectives. Chapter 4 includes the results of the bathymetric and transport analyses. A discussion of the results is presented in Chapter 5 and Chapter 6 holds the conclusions for this study. The study contains an appendix and a reference list as well.

2. Literature review

2.1 Shoreface transport mechanisms

2.1.1 Cross-shore transport

In order to be able to explain bathymetric changes on the shoreface, it is important to understand the underlying transport mechanisms. In this section the transport processes are discussed for the shoreface. Whereas this study focuses on the lower shoreface, it was chosen to include the upper shoreface here as the upper and shoreface are coupled in terms of the dynamics (Hinton & Nicholls, 2007) and the extent of some of the processes is of not entirely restricted to either the upper or the lower shoreface.

As mentioned before, the upper shoreface is much more active in terms of morphodynamics and on shorter timescales compared to the lower shoreface. The upper shoreface encompasses the depth range including the surf and swash zone. Therefore, the bed is frequently agitated by wave effects. Large sediment transport rates therefore occur on the upper shoreface, especially during storm events (e.g. Anthony, 2013; Backstrom et al., 2009; Castelle et al., 2015; Holman et al., 1978; Loureiro et al., 2012; Thornton et al., 2007; Vidal-Ruiz & Ruiz de Alegría-Arzaburu, 2019; Witteveen, 2012). On the upper shoreface, the direction and magnitude of cross-shore sediment transport are determined by the combination of mechanisms that have been studied extensively (Aagaard, 2011; Aagaard & Greenwood, 1994; Aagaard & Kroon, 2007; Backstrom et al., 2009; Baldock, Manoonvoravong, & Pham, 2010; Battjes, Bakkenes, Janssen, & Van Dongeren, 2004; Bertin et al., 2018; De Bakker, Herbers, Smit, Tissier, & Ruessink, 2015; Hassan & Ribberink, 2005; Hoekstra et al., 1997; Hsu, Elgar, & Guza, 2006; Knook, 2013; Mariño-Tapia, Russell, O'Hare, Davidson, & Huntley, 2007; Navas, Cooper, Malvares, & Jackson, 2001; Nielsen, 2006; Reniers, Macmahan, Thornton, & Stanton, 2006; Ruessink, Houwman, & Hoekstra, 1998; Ruessink, Ramaekers, & Van Rijn, 2012; Van Rijn, 1997; Verschure, 2014; Witteveen, 2012).

Much less attention has been attributed to the lower (Hamon-Kerivel et al., 2020). Similar to the upper shoreface, waves and mean currents induce cross-shore transport on the lower shoreface (Aagaard, 2011; Backstrom, et al., 2009; Héquette et al., 2008). However, the rates of sediment transport are much lower resulting in slower adaptations of the sea bed (e.g. Vermaas et al., 2015). The impact of waves diminishes towards the lower shoreface and hence wave-driven transport as well (e.g. Aagaard, 2014; Héquette et al., 2008; Kleinhans & Grasmeijer, 2006; Knook, 2013). Transport on the shoreface is often dominated by currents

however waves mobilize the sediment and may contribute significantly to the net transport (King et al., 2019; Kleinhans & Grasmeijer, 2006; Van Dijk & Kleinhans, 2005). Wave skewness, up- and downwelling by wind-induced, density-induced currents and return currents determine the cross-shore transport on the lower shoreface (e.g. Aagaard, 2011, 2014; Backstrom et al., 2009; Grasmeijer, 2018; Grasmeijer et al., 2022; Knook, 2013; Loureiro et al., 2012; Ortiz & Ashton, 2016; Patterson & Nielsen, 2016; Stive & de Vriend, 1995; van Rijn, 1997).

The following cross-shore transport mechanisms are present on the shoreface:

- Wave skewness (onshore transport) – the onshore directed orbital velocities under a wave slightly exceed those offshore, resulting in a net-onshore transport. This increases with decreasing water depth and is thus variable in the cross-shore. Low-sloping shorefaces also result in larger transport by wave skewness.
- Wave streaming (onshore transport) – Waves induce a current in the direction of wave propagation in the boundary layer close to the bed. This increases with decreasing water depth and is thus variable in the cross-shore. Similar to wave skewness, it increases with decreasing water depth. Low-sloping shorefaces also result in larger transport by wave skewness.
- Return currents (offshore transport) – Onshore propagating waves and surges transport of water to the shore. This causes the formation of return currents (undertow and rip currents) to balance this onshore transport in mass. The magnitude is dependent occurs primarily in the zone of wave breaking and is slope-dependant. It thus increases during storms. Steep sloping shoreface generally tend to enhance offshore transport by return currents.
- Wind-induced currents (offshore/onshore transport) – Onshore (offshore) winds drive an onshore (offshore) surface current. To balance this in terms of mass conservation, a bottom return current is often present causing net-transport in one direction. This is called upwelling/downwelling based on the direction.
- Density-induced currents (onshore transport) – Stratification near freshwater outflows may cause the formation of a low-density lens on top of dense seawater. The lateral expansion of this lens is balanced by a bottom current towards the shore, causing net onshore transport.
- Infragravity waves (onshore/offshore transport) – Infragravity waves generate currents that interact non-linearly with stirred sediment by incident waves. This results in onshore or offshore transport depending on the conditions and water depth and occurs primarily in the surf and swash zone during storms, close to the beach.

The hydrodynamic sediment transport processes on the upper shoreface have been measured frequently in the field during all sorts of conditions or in laboratory environments (Baldock et al., 2010; Battjes et al., 2004; De Bakker et al., 2015; Hassan & Ribberink, 2005). This allows for a good quantification of the above cross-shore processes on the upper shoreface. The data from field measurements (e.g. Witteveen, 2012) have been used widespread to set-up good-functioning and quite accurate models (Giardino et al., 2010; Huisman et al. 2019, 2018; Roelvink et al., 2009; Ruessink et al., 1998).

Cross-shore transport on the lower shoreface has been poorly quantified (Aagaard, 2014). Several challenges complicate studying processes on the lower shoreface. Upscaling the short-term transport processes to large temporal and spatial scales faces challenges such as including non-linear behaviour (e.g Aagaard, 2014; de Boer, 2009; Van de Meene & Van Rijn, 2000). Modelling results depend heavily on the hydrodynamic input and the probability of the conditions (e.g. Grasmeijer et al., 2022; Kleinhans & Grasmeijer, 2006). To cope with such processes lower shoreface transport and hydrodynamic processes are often parametrised and as a result the model results are uncertain (e.g. Aagaard, 2014; Kleinhans & Grasmeijer, 2006; Ortiz & Ashton, 2016; Ruessink et al., 2012; Stive & de Vriend, 1995). Besides, the relative contribution of the different mechanisms cannot be derived from parametrized models because they are not process-based. In other cases transport mechanisms are not implemented in the models, e.g. Knook (2013) excluded density-driven currents in their model. Bathymetric measurements and budget studies are a solution to the above challenges to understand how transport processes affect the lower shoreface such as for Backstrom et al. (2009). However, the data coverage of bathymetric measurements is often too limited in terms of spatial extent and/or temporal resolution such as for van Rijn (1997) and Walburg (2005). On a smaller scale, there is a lack of data of the lower shoreface processes because measuring transport is difficult (da Motta, Toldo, de Almeida, & Nunes, 2015; Kleinhans & Grasmeijer, 2006) since installing and retrieving measuring equipment is more difficult in large water depths (Anthony & Aagaard, 2020). Consequently, shoreface research has been heavily focused towards the upper shoreface whereas the lower shoreface is under reviewed in terms of sediment transport.

2.1.2 Longshore transport

Longshore transport on the shoreface may be dominant over cross-shore transport (Grasmeijer et al., 2022; Héquette et al., 2008; Kleinhans & Grasmeijer, 2006). This is the case for the Holland coast as well. With that it is important to know the current state of knowledge of longshore transport mechanisms as well.

Wave-driven currents generally dominate the alongshore transport on the upper shoreface, especially in cases where to propagate obliquely to the shoreline. In some cases wind strongly affects the longshore transport (Aagaard, 2011; Grasmeijer et al., 2022; Héquette et al., 2008). Towards the lower shoreface wave-driven transport diminishes (Patterson & Nielsen, 2016) and (net) transport due to the tide becomes dominant (Grasmeijer et al., 2022; Héquette et al., 2008; Kleinhans & Grasmeijer, 2006; Van de Meene & Van Rijn, 2000).

On shoreface scales, longshore transport is sometimes determined as an input or output value to assess the sediment budget of the shoreface (Aagaard, 2011; Brunel et al., 2014; da Motta et al., 2015; Hapke et al., 2010). Though, it is difficult to measure longshore transport (da Motta et al., 2015) and hence the longshore transport values are therefore mere estimates and consequently include uncertainty (Hapke et al., 2010). On smaller scales, measurements have contributed to our knowledge of the local conditions (Aagaard, 2011; Héquette et al., 2008; Kleinhans & Grasmeijer, 2006; Van de Meene & Van Rijn, 2000) and models predict the hydrodynamics and transport processes with reasonable accuracy, mostly on cross-shore profile or nourishment scales (e.g Giardino, van der Werf, & van Ormondt, 2010; Grunnet, Walstra, & Ruessink, 2004; Hoekstra et al., 1997; B. G. Ruessink, Miles, Feddersen, F.Guza, & Elgar, 2001). However, most studies focus on the upper shoreface again most of the time. Additionally, studies that describe alongshore transport on the shoreface either focus on the sediment budget of an entire coast (Aagaard, 2011; Brunel et al., 2014; da Motta et al., 2015; Hapke et al., 2010) or on scales much smaller (a single location, cross-shore profile or a nourishment) (Giardino et al., 2010; Héquette et al., 2008; Hoekstra et al., 1997; Kleinhans & Grasmeijer, 2006; Ruessink et al., 2001). There is only a limited amount of studies about the effects of longshore transport on a scale in between (i.e. for different locations along a shoreface): Grasmeijer et al. (2022) and van Rijn (1997) studied alongshore variations in alongshore transport at different locations along the Dutch coast and Aagaard (2011) along the Danish coast. They all show that transport gradients are significant along a coastline. In the case of van Rijn (1997) and Aagaard (2011) they are explanatory for observed sediment volume changes along the shore in combination with cross-shore transport. The longshore transport gradients and their effect on shoreface bed level changes should therefore not be neglected. The results of Grasmeijer et al. (2022) have not been validated in a morphodynamical sense yet. However, the the hydrodynamic output was validated and showed a good reprentation of the observed conditions.

2.2 The shoreface of the Holland coast

This study focuses on the shoreface of the Holland along the Dutch closed barrier coast. In this section, we elaborate on this research area specifically to determine the existing knowledge about sediment transport and bed level changes.

2.2.1 The Holland coast

Van der Werf et al. (2017) performed an extensive literature study of the Dutch shoreface, which is very useful for this study. We refer to them for a more extensive literature study. The study area of this study encompasses the lower shoreface of the closed barriers coast of Holland. This is the zone between -20 (the seaward limit of the coastal foundation) and -10 m depth contour, see the yellow box in Figure 1. The lower shoreface has a variable width along the shore. At the south, it is around 5 km wide. In the central part is around 12 km wide and diminishes again towards the north where it has a width of roughly 6 km. The lateral ends of the lower shoreface are bordered by the Zeeland estuaries including the Meuse and Rhine river mouths in the south and by the Texel inlet of the Wadden in the north. The Noordzeekanaal splits the barrier coast in a northern and southern part. At the central part of the coast, a zone of shoreface-connected ridges is present (Van de Meene & Van Rijn, 2000). The closed barrier coast formed when the sea level rise levelled out during the Holocene around 5000 BP and the coast went from a retreat towards a stable coast (Van der Werf et al., 2017). The inlet systems from the period of coastal retreat were filled with sediments and due to peat formation and a barrier could form, closing the coastline. The shoreface geology consists of Holocene and Pleistocene sediments and with that it there is abundant sediment available for transport (Van der Werf et al., 2017).

2.2.2 Hydrodynamic and wind conditions

The hydrodynamics are the driving forces behind sediment transport and hence bed level changes. The general hydrodynamic setting is therefore briefly described in this section. The knowledge on the hydrodynamics on the Dutch lower shoreface has progressed sufficiently and models have been developed to simulate the hydrodynamics with small errors only (e.g. Grasmeijer et al., 2022; Zijl et al., 2018). The hydrodynamics on the lower shoreface of the Holland coast include waves, wave-driven currents, tidal currents, wind-induced currents and density-driven currents (Van der Werf et al., 2017). The tidal range decreases from 1.76 near Scheveningen to 1.60 m near Callantsoog (Van der Werf et al., 2017). The combination of currents results in alongshore currents. Semidiurnal tides propagate from south to north and

due to interaction with the shoreface and shelf, the waves develop an increasing tidal asymmetry towards the north (Dronkers, 1986; Grasmeijer et al., 2022). The flood currents dominate over the ebb currents, hence resulting in northward directed depth-averaged residual currents. These are primarily directed along the shore. The ratio of maximum flood currents over the sum of maximum flood and ebb currents increases northward from 0.57 at offshore of Scheveningen to 0.60 offshore of Callantsoog (Grasmeijer et al., 2022). On the upper shoreface, tidal currents diminish towards shallow water depths and wave-driven alongshore currents dominate (Giardino et al., 2010; Ruessink et al., 2001). The wave and wind regime includes a dominant southwestern direction and wave heights increase northwards from a mean significant wave height of 1.06 m offshore at Scheveningen to 1.19 m offshore at Callantsoog. In the North, the tidal currents near the Texel are probably slightly affected by tidal inlet processes according to Elias & Van Der Spek (2017). Storms events are important in the study area and may cause large increases in the significant wave height (up to 7 m offshore at Egmond), especially when the wind blows from the northwest (de Winter et al., 2015). The hydrodynamics are influenced by an annual fresh water supply of 2500 m^3/yr of the Rhine-Meuse river mouths at the southern end of the coast (de Boer, 2009). It creates a stratified plume along the shore with dense salt water at the bottom and a freshwater lens on top. The extent of this plume is variable based on the mixing conditions and may cover nearly the entire shoreface of the Holland coast. This results in a radial seaward flow at the sea surface and balancing onshore-directed bottom currents (upwelling). Onshore winds counteract and offshore winds reinforce this effect (Van de Meene & Van Rijn, 2000). Whereas the annual depth-averaged residual currents were calculated to be dominated by the tide, near-bed residual velocities were primarily onshore due to the effects of density and wind (Grasmeijer et al., 2022).

2.2.3 Sediment transport

Such as stated earlier, transport is generally poorly quantified on the lower shoreface. This subsection focuses on lower shoreface transport for the Holland coast to determine what the current state of knowledge is for this area.

Local sediment transport on the lower shoreface of Holland was determined by Kleinhans & Grasmeijer (2006) and Meene & Van Rijn (2000). Kleinhans & Grasmeijer (2006) developed a bedload transport predictor in water depths using hydrodynamic measurements between 13-18 m water depth near Noordwijk. Waves are important for mobilizing sediment and promote gross transport by tidal currents. Waves were relatively unimportant for net transport however,

which was in the direction of the tidal flood currents. The prediction model showed much lower bed load transport rates compared to other studies such as an Rijn (1997).

Similar transport mechanisms were observed by van de Meene & Van Rijn (2000) for both bedload and suspended load at a similar water depth at Zandvoort on top of a shoreface-connected ridge. During fair weather conditions, transport primarily occurred in a 2-hour window around the peak tidal currents when the currents exceeded a threshold value for transport. During storm conditions, waves stirred sediment more easily and transport was dominated by mean fluxes. Density driven-residual currents resulted in a secondary onshore transport component.

Knook (2013) studied cross-shore transport along a cross-shore profile of the shoreface at Noordwijk for the 5 m depth contours. The effect of density is excluded from the Unibest-TC transport model when in fact density effect on sediment transport has been found to be non-neglectable on the Holland shoreface (Grasmeijer et al., 2022; Van Rijn, 1997). Nonetheless, their model results show net onshore transport comminated by waves and offshore transport comminated by return currents on the lower and upper shoreface, respectively. Adding waves with a variable angle and tidal currents reversed this pattern and caused offshore transport dominated by the tidal currents on the lower shoreface and onshore wave-related transport on the upper shoreface.

Van Rijn (1997) and Grasmeijer et al. (2022) set up models to simulate the longshore and cross-shore transport for the shoreface of Holland and the entire Dutch coast, respectively. Van Rijn (1997) set up a combined known sources and sinks of sediment with gradient-driven transport formulations. Their calculations identify density-driven currents as the dominant transport mechanism for cross-shore transport at the seaward boundary of the shoreface at 20 m water depth. Transport induced by wave skewness effect, infragravity waves, Longuet-Higgens streaming and return currents is negligible according to their calculations on this boundary. In 8 m water depth, these mechanisms are much more important and density-driven currents were the weakest mechanism. However, the cross-shore transports at the 8 m water depth were uncertain. The longshore transport increases northward and is nearly restricted to the surf zone near the breaker bars, although the annually integrated value show large uncertainties.

Grasmeijer et al. (2022) computed annual transport rates at the Dutch lower shoreface using a Delft3D model. The modelled transports of Grasmeijer et al. (2022) have not been validated yet morphodynamically. The transport rates show that the tidal asymmetry is dominant and results in an increasing alongshore transport towards the north. Through a sensitivity analysis, they showed that density- and wind-effects significantly affected the transport. Density-effects

promoted onshore transport and counteracted longshore transport towards the north. Wind effects diminished onshore transport and reinforced longshore transport towards the north. The sensitivity of return currents was tested as well. Including return currents reduced annual transport across the seaward boundary at 20 m water depth with 11-20 percent. This is in contrast to van Rijn (1997) who estimated that return currents were negligible at such water depths. Variable conditions for the years studied (2013-2017) also resulted in variable transports across the boundary at 20 m water depth, showing the importance of the forcing hydrodynamic conditions.

There is clearly no agreement on the magnitudes and importance of transport mechanisms for the shoreface of the Holland coast. The different studies indicate different magnitudes and the dominant transport mechanisms differ. This is probably the result of different approaches and/or because different sites were studied at different times where the conditions differ. Comparing results derived from different locations, at different times and with different methods should be done very carefully to avoid the apparent differences in the sediment transport magnitudes. To solve this problem it is recommended to apply a single method to the entire shoreface of Holland such as for the model studies of van Rijn (1997) and Grasmeijer et al. (2022).

2.2.4 Local and regional morphodynamics

Studying the bed level changes and understanding the processes responsible requires a basal knowledge of the morphodynamics of the studied area. Here the currents knowledge is explained about the morphodynamics of the Holland shoreface. These are split into local/regional and large-scale (= shoreface scale) morphodynamics.

The central part of the shoreface near the Noordzeekanaal is affected by a large field of shoreface-connected ridges with a SW-NE orientation. However, it is not certain how these morphodynamic features affect the sediment on the lower shoreface of Holland (Spek et al., 2020). They seem to be affected by a combination of the persistent tidal currents along the shore and waves during storm events (Van de Meene & Van Rijn, 2000). Hence, their orientation is not entirely the same as the dominant tidal currents. The shoreface-connected ridges propagate northward with the tidal currents however, meaning that accumulation occurs at the north and erosion at the south of the ridges. These dynamics result in dropping and rising bed levels on the central part of the lower shoreface.

In the same region, sand waves with amplitudes over a meter are superimposed on the shoreface-connected ridges (Van Dijk & Kleinhans, 2005). At 14-18 m water depths, waves

stirred tidal currents moved the sediment, resulting in large migration rates. Offshore in 26-30 m water depths, the effect of waves was restricted to storm events only, hence the migration rates were much smaller. Similar to the shoreface-connected ridges, the movement of these features induce bed level variations in the sandwave regions (Van Dijk & Kleinhans, 2005; Vermaas et al., 2015).

The morphodynamics of the Holland shoreface are anthropogenically affected. Harbour seawalls and groynes on the upper shoreface in shallow water induce flow convergence and with that erosion of the deep part of the upper shoreface and also the upper part of the lower shoreface. This has a steepening effect the middle part of the shoreface (Van Rijn, 1997).

Shoreface nourishments occur on the upper shoreface shoreward of -10 m according to Huisman et al. (2019). They studied the evolution of large number of shoreface nourishments. The zones seaward of the nourishments also showed a decrease in the sediment volume indicative of erosion. This is the cause of increased wave skewness and consequential onshore transport seaward of the nourishment zones. Thus, the upper part of the lower shoreface is prone to this effect. Mega nourishments such as the Sandmotor extend further seaward even onto the lower shoreface and thus induces artificial bed level changes. Because the convergence of flow, this results in increased alongshore transport at the tip of the mega nourishment and thus erosion (= decrease in bed level) (Huisman et al., 2018). For the Hondschbosche Duinen mega nourishment, such effects are not yet studied but assumed to be similar.

2.2.5 Large-scale morphodynamics

Via bathymetric measurements, the largescale morphodynamics and evolution of shoreface has been addressed in multiple studies (Hinton & Nicholls, 2007; Spadon, 2000; Van Rijn, 1997; Walburg, 2005).

Hinton & Nicholls (2007) studied the bed level changes on the shoreface of the Holland coast. They indicated that morphodynamic activity occurs in deep water levels on the lower shoreface as well, especially on larger temporal scales (i.e. a decade). Moreover, they showed that the upper and lower shoreface were coupled in terms of bed level changes and that the lower shoreface generally showed a decrease in bed level due to a constant onshore flux of sediment.

The bed level change along cross-shore profiles was also investigated by Spadon (2000). He analysed the movement of depth contours to determine erosion and sedimentation trends. Based on this analysis, he showed that the zone between -14 and -8 m water depth was prone

to erosion. This is consistent with the findings of Hinton & Nicholls (2007). This resulted in deepening of the lower shoreface and steepening of the cross-shore profile since the shoreline is fixed due to nourishments.

The transport-based results of the morphodynamic evolution of a cross-shore profile such as modelled by Knook (2013) also indicated shoreface steepening and lower shoreface deepening in the case a tidal current and variable wave angle was included. Offshore transport on the lower shoreface and onshore transport on the upper shoreface caused this steepening and deepening effect.

Vermaas et al. (2015) studied the range and rates in bed level changes for the Dutch lower shoreface. The bed level changes diminished towards the lower shoreface for the Holland coast and the mean changes were roughly 0 seaward of 10 m water depth for both Noord-Holland and South-Holland. This is different compared to the previously mentioned studies of Spadon (2000) and Hinton & Nicholls (2007) who identified a negative trend in the bed level for the lower shoreface. Maybe this related to differences in data between Vaklodingen/JARKUS and that of the Hydrografische Dienst.

The lower shoreface is found to deepen and the shoreface slope is found to steepen in the middle part because vast amounts of sediment have been nourished over the past decade to counteract coastal recession and to fix the shoreline. From the transport section, the net transport direction was found to be slope-dependant. The steepened slopes on the shoreface of the Holland coast may eventually affect the balance between onshore wave-related transport and offshore transport by return currents and trigger a reversal of the net transport direction. It would be interesting to model shoreface transports for two different bathymetries (original versus steepened shoreface) to discover the effects of this. The mega nourishments are a relatively new management technique to assure that the coastal foundation contains enough sediment. However, nourishing such large amounts of sediment may cause a local excess of sediment and dispersal to the lower shoreface. It is therefore uncertain how they affect the bed levels on the lower shoreface.

3. Methods

3.1 Research area

The study area is the lower shoreface for the Holland coast of the Netherlands. An extensive description of the study area can be found in the literature review. The boundaries of the study area are similar to the nearshore zones described by Vermaas et al. (2015), see left of Figure 2. The -20 m NAP contour is the seaward boundary. The landward boundary was moved to -10 m NAP contour to exclude the effect of shoreface nourishments. This closed barrier coastline is selected to minimalise tidal inlet processes from the Zeeland estuaries in the south and from the Texel inlet in the north. The study area is split into a northern and southern section by the Noordzeekanaal (see Figure 2). The study area is a sandy environment with grain sizes between 250 and 300 μm (Van der Werf et al., 2017).

The northern and southern sections are each divided into three separate zones (Figure 2), both cross-shore longshore and are coded N and S. The orientation of the coastline was determined from taking 14 JARKUS section orientations along the coast: both at the boundaries and in the middle of each longshore zone, depicted as the red triangles in Figure 2. Moreover, the grid of the transport data is shown.

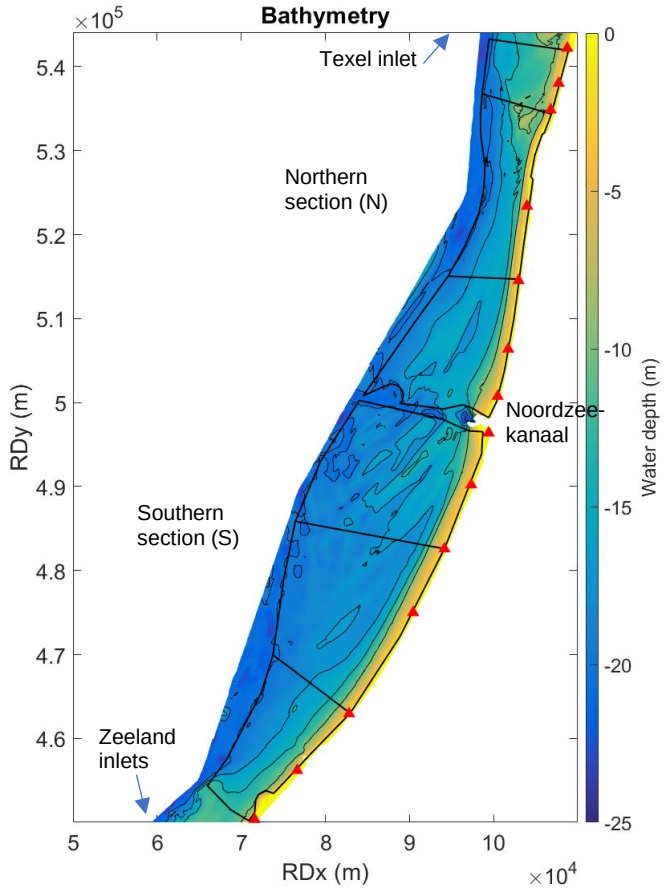

Figure 2: The bathymetry, longshore zones and JARKUS sections (left) and the transport grid and the coastal orientation (right).

3.2 Bathymetric data and sediment volumes

3.2.1 Vaklodingen data

The bathymetric data is retrieved from the Vaklodingen dataset. It is measured and processed by Rijkswaterstaat in 12.5x10 km rectangular tiles of the Dutch coastal waters called Vaklodingen. The data reaches down to a water depth slightly over -20 m NAP. The data has a spatial resolution 20 m. The temporal resolution is different for sections of the Dutch coasts and varies between 1 to 6 years. The data fully covers the study area in the period between July 2005 and January 2017. The time window of the analysis was narrowed down to 2009-2017 because of an unknown data error in the measurements of 2005 (see Appendix A).

The measurements for different sections of the study were carried out at different times, resulting in a mosaic of data, such as for Walburg (2005). Resampling of the data to equal moments in time was required. The bathymetry was therefore interpolated linearly between the available measurements for each grid cell to four queried time points per year (1 January, 1 April, 1 July and 1 October). The number of available measurements present in the studied

period between 2009 and 2017 is shown in Figure 3. Interpolation to a finer temporal resolution demanded too much computing power because of the fine spatial resolution of the data (20x20 m). Because of the slow sediment transport rates on the lower shoreface, it assumed that linear interpolation causes small errors only and that long-term trends are captured in the data anyway.

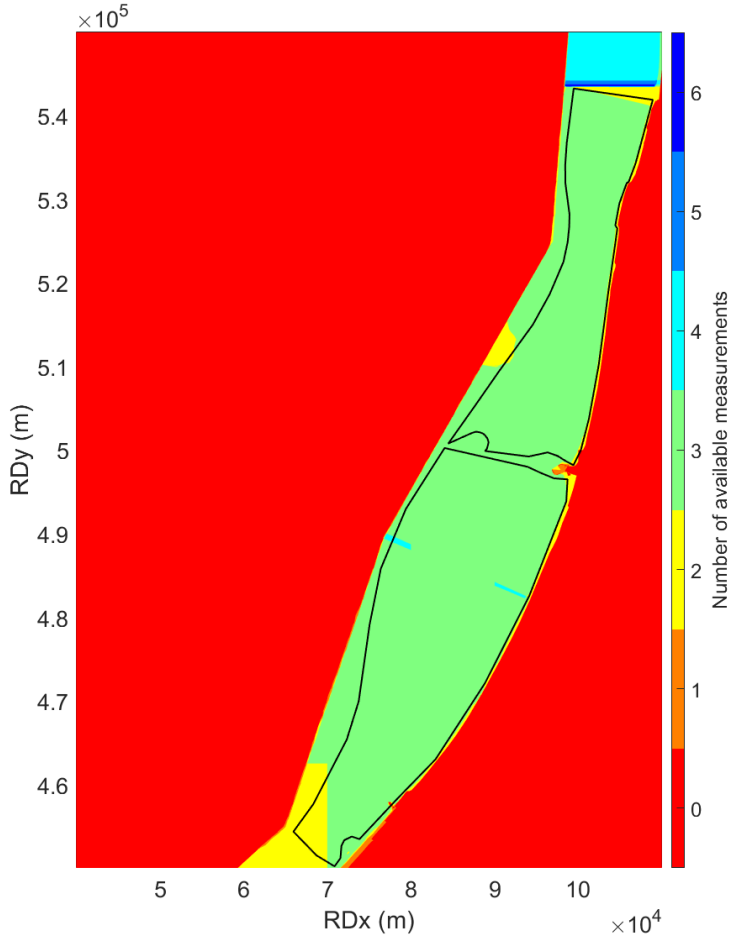

Figure 3: Number of available Vaklodingen bathymetric measurements in the study area between 2009-2017

I refer to Wiegman et al. (2002, 2005) for an elaborate description of measuring and calibration accuracy and errors regarding the use of Vaklodingen data. A part of these errors show stochastic behaviour and level out on the scale of entire coastlines (Walburg, 2005) so the effect for the results is this study are minor. Systematic errors are introduced due to the innovation of measuring equipment and calibration techniques. The systematic errors induce false bathymetric changes and may affect the results of this study. This will be further discussed in the Discussion section. The bathymetric data clearly contains outliers in 2005 and these are interpolated to the period between 2005 and 2009 (Appendix A). A rectangular patch of grid cells orthogonal to the shoreline extends from the coast to the seaward boundary at -20 m and shows an anomaly. Analysis pointed out that a number of transects 2005 included a negative bias (underestimation) in the water depth roughly between 35 and 40 cm. Through

interpolation, this results in a patch of underestimated water depths. The measurement from 2005 is therefore discarded and excluded from our analyses.

3.2.2 Data analysis

The bathymetric changes are determined between 2009 and 2017 for each cross-shore and longshore zone. The northern and southern section are each divided into three cross-shore zones (shallow, intermediate and deep), based on the most recently measured water depth (January 2017). Table 1 shows the depth ranges that are used. The longshore zones are also labelled. Table 2 shows the labelling for these zones, signified with an N (northern section) or S (southern section) and a subscript. The characteristics of 14 JARKUS sections used for the coastal orientation are also used and labelled in the same table.

Table 1: Cross-shore zone labelling based on the water depth.

Label	**Depth range (m NAP)**
Shallow	-10 to -14
Intermediate	-14 to -17
Deep	-17 to -20

Table 2: Longshore zone plus transect labelling and JARKUS characteristics for the 14 used sections.

Type	Label	Jarkus transect ID	RDx (m)	RDy (m)	Orientation (°)	Length (km)
Transect	N_{north}	7000994	108770	542203	284	9.09
Zone	N_{north}	7001421	107751	538036	286	-
Transect	N_{north}- N_{centre}	7001755	106788	534840	287	8.82
Zone	N_{centre}	7002935	103982	523387	276	-
Transect	N_{centre}- N_{south}	7003825	102978	514535	278	8.01
Zone	N_{south}	7004650	101737	506367	282	-
Transect	N_{south}	7006225	100493	500749	283	17.42
Transect	S_{north}	8005675	99418	496379	287	14.79
Zone	S_{north}	8006325	97344	490200	291	-
Transect	S_{north}- S_{centre}	8007150	94164	482582	293	17.54
Zone	S_{centre}	8008000	90433	474982	298	-
Transect	S_{centre}- S_{south}	8009425	82816	462942	309	10.97
Zone	S_{south}	9010338	76647	456197	311	-
Transect	S_{south}	9011109	71586	450361	310	5.97

A comparison was made between the changes in sand volumes on the shoreface determined from the bathymetry and between a transport-based method. To do this, the bathymetric changes were converted to sediment volumes using the surface areas of the zones, listed in Table 3 in km^2. The bathymetry was here taken between 2013 and 2017 to match the period of the transport data (Grasmeijer et al., 2022).

Table 3: Surface areas of the longshore and cross-shore zones for both analysis in km^2.

	$N_{shallow}$	$N_{intermediate}$	N_{deep}	$S_{shallow}$	$S_{intermediate}$	S_{deep}
Cross-shore zones	67.9	148.1	97.9	67.7	159.7	364.6
	N_{north}	N_{centre}	N_{south}	S_{north}	S_{centre}	S_{south}
Longshore zones	183.6	123.3	61.6	247.3	275.7	140.3

3.3 Transport data

The transport data was derived from Grasmeijer et al. (2022). They modelled the transport for the period between 2013 and 2017 on the Dutch shoreface by combining the 3D Dutch Continental Shelf Model with Flexible Mesh model (3D DCSM-FM-model) with a wave transformation method and a 1-dimensional vertical (1DV) transport model. We refer to (Grasmeijer et al., 2022) for a more extensive description of the approach.

The 3D DCSM-FM model computes water levels, currents, salinity and temperature on the North Sea shelf on various temporal and spatial scales by solving the shallow-water equations for 20 vertical layers each from 5% water depth in the water column. The vertical resolution thus increases in shallow regions. 33 tidal constituents were used from the FES2012 model to force the hydrodynamics at the open boundaries. The model includes river discharges as well as meteorological effects on the water surface, e.g. by wind and air pressure variations. The meteorological parameters were obtained from the Hirlam7.2 model. The Hirlam7.2 resolution is about 840 by 930 m near the Dutch coast and decreases towards larger water depths. The 3DCS-FM model water levels were validated for 13 stations along the Dutch coast. The root-mean-square-error (RMSE) in the water levels was 9-10 cm. Moreover, the model currents speeds were validated by comparing two offshore stations 27 and 28 km from the coast of Egmond aan Zee. The model overestimated current speeds up to a maximum of 7 cm/s.

The wave input was derived from a wave transformation matrix. A set of 269 different observed offshore conditions, divided into classes of wave height, period and directions was used to

simulate the wave transformation across the Dutch shoreface using SWAN. These simulations were used to determine transformation factors for the wave (height, peak period and direction), wind properties (speed and direction) and the surge. Consequently, the wave conditions on the shoreface can easily be computed from offshore conditions.

To compute transport, a 1DV (one-dimensional vertical) TSAND model was used based on the approach from van Rijn (2007a,b). The transport model is suitable for sandy environments such as the Dutch shoreface. The transport model determines total transport as the sum of depth-integrated suspended load and bedload transport:

$$q_s = \sum_{a}^{h} (uc) dz$$

$$q_b = \int_0^T q_{b,t} dt$$

$$q_{tot} = q_s + q_b$$

In which q_s is the suspended load transport, h the water depth, a the reference height above the bed, u the current speed, c the concentration of suspended load, q_b the bedload transport, T the wave period, $q_{b,t}$ the intra-wave time-dependant transport and q_{tot} the total transport.

The cross-shore and longshore zones were used as well to determine the mean transport in each of the zones. Moreover, the transport was decomposed into a longshore and cross-shore component using the coastal orientation based on the 14 JARKUS sections. The coastal orientations were extrapolated to the grid points of the transport model, as shown in Figure 4.

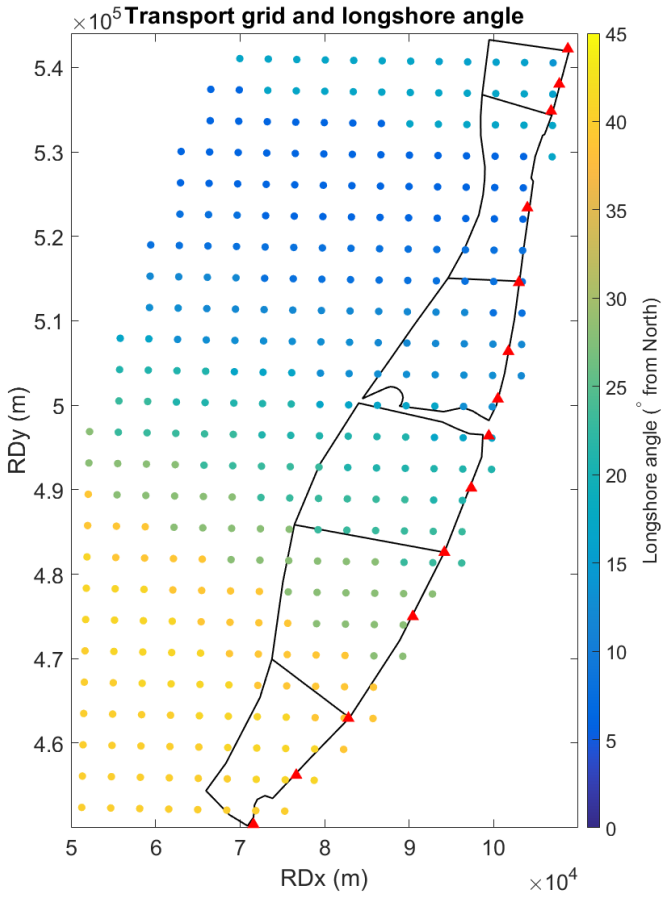

Figure 4: JARKUS-based orientation of the transport model grid points.

4. Results

4.1 Bathymetric changes

This section presents the mean bed level changes between 2009 and 2017 in the cross-shore and alongshore zones. Note that the colour axis is variable for the different figures.

4.1.1 Cross-shore analysis

Figure 5 shows the mean bed level changes between 2009 and 2017 for the cross-shore zones. Deep, intermediate and shallow refer to the depth ranges of -20 to -17, -17 to -14 and -14 to -10 m NAP, respectively (see Table 1). The entire northern section showed net erosion with larger erosion values near the shore. The southern section was prone to seaward accumulation in S_{deep} and $S_{intermediate}$ and accumulation in the shallow part of the lower shoreface. The difference between the cross-shore zones is therefore larger for the southern section. This is consistent with Vermaas et al. (2015) who showed that range in bed levels is larger for Zuid-Holland compared to Noord-Holland. The observed bed levels in the cross-shore zones are indicative of flattening of the lower shoreface. For the northern section this is the result of increased deepening in the shallow part of the lower shoreface. For the southern section, this is due to deepening of the shallow part of the shoreface in combination with accumulation on the deep part of the shoreface. In other words, the flattening is largest on the southern section of the lower shoreface. Our results are contrasting with those of (Spadon, 2000) who indicate a steepening of the lower shoreface. The shoreface deepening such as observed by Hinton & Nicholls (2007) and modelled by Knook (2013) only partially agrees with this study: for North-Holland Steepening of the shoreface in its entirety is likely: the upper shoreface remains fixed due to nourishments (e.g. Brand et al., 2022) and the upper part of the lower shoreface erodes according to the bathymetric results.

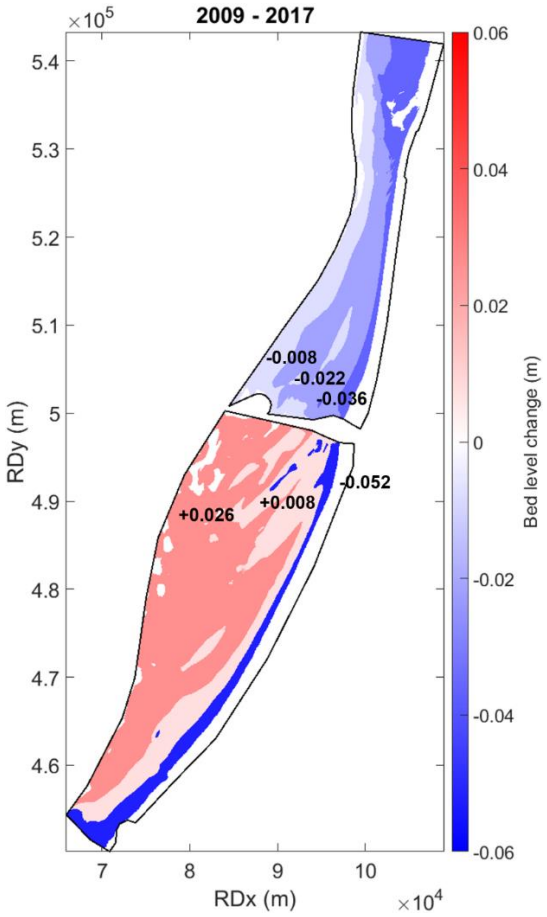

Figure 5: Mean bathymetric changes between 2009-2017 in the cross-shore zones between -20 and -10 m NAP.

4.1.2 Longshore analysis

Bed level changes for longshore zones were determined as well and are presented in a similar manner to those for the cross-shore zones. Figure 6 presents the mean bathymetric changes in the period 2009 to 2017 for the longshore zones. The mean bed level changes are variable alongshore. The zones of N_{north} and N_{centre} were prone to erosion. As a consequence, the mean bed levels decreased in N_{north} and N_{centre}. Accumulation occurred on the middle part of lower shoreface of Holland hence showing an increasing mean bed level in N_{south} and S_{north}. Changes in the lower section of the Holland coast were small: the bed level slightly decreased in S_{centre} and increased in S_{south}.

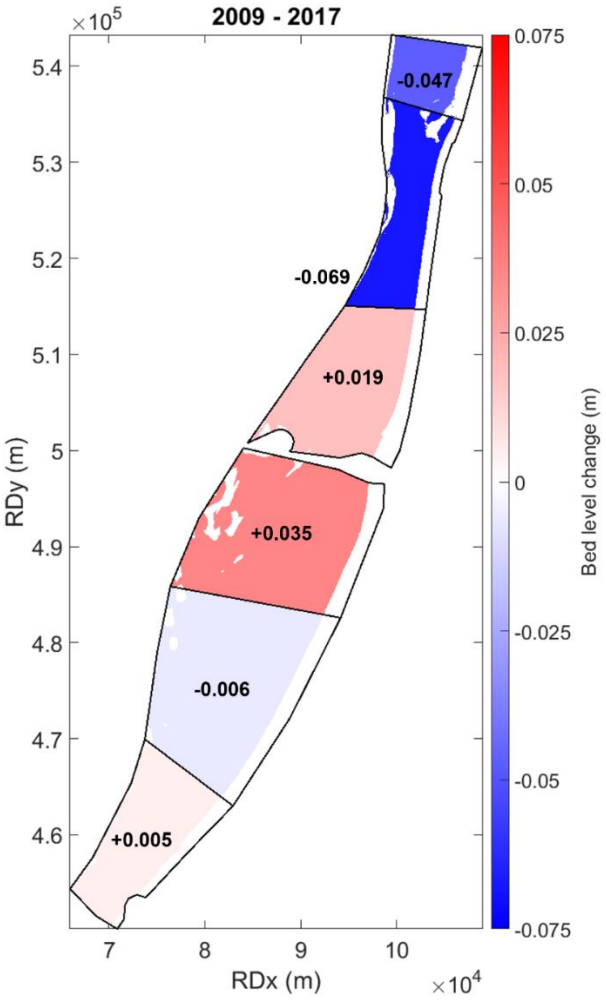

Figure 6: Mean bathymetric changes between 2009-2017 in the longshore zones between -20 and -10 m NAP.

4.1.3 Local bed level changes within the zones

Figure 7 shows the internal bed level changes within the zones between 2009 and 2017. For this figure, it was chosen to include the upper shoreface to show the impact of the mega nourishments and harbour seawalls. It can be observed that the bed level changes are much larger than the mean bed level changes in Figure 5 and Figure 6. Strong accretion is observed generally close to the shore, especially in N_{centre} and in S_{north} close to the IJmuiden harbour. These changes are due to frequent nourishments on the upper shoreface (e.g. Brand et al., 2022; Quataert et al., 2021; Huisman et al., 2019) and due to the harbour seawalls (Schuiling, 2019; Van Rijn, 1997). Large changes occur in deep water in S_{centre} and S_{north} both as regions of erosion and accretion. The area is known to be affected by shoreface-connected ridges in combination with sandwaves (Van de Meene & Van Rijn, 2000). The dynamics are likely to be related to this such as found by Vermaas et al. (2015). Slight decreases in bed level occur

generally in the deeper parts of N_{north} and N_{centre} whereas widespread accretion is measured in the region of N_{south}.

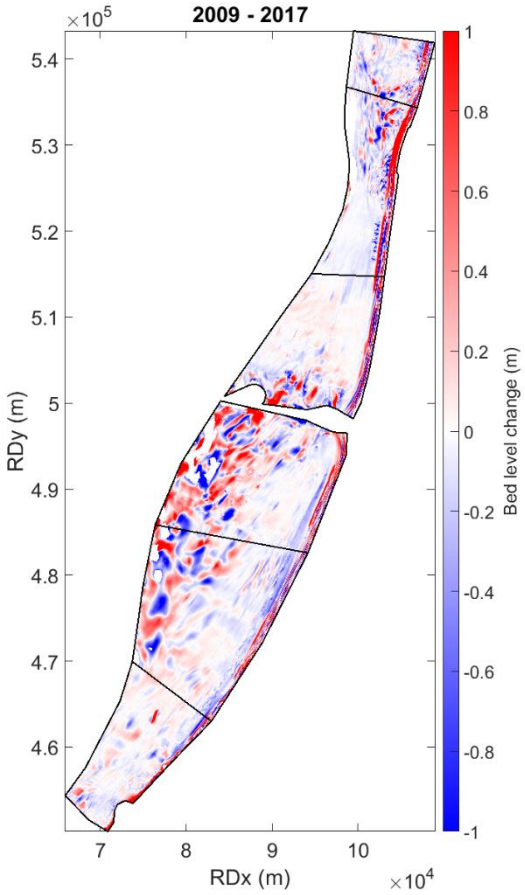

Figure 7: Bathymetric changes between 2009-2017.

4.2 Sediment transport

Transport data was derived from process-based simulations using the 3D DCSM-FM-model, a wave transformation method and a 1DV transport model (Grasmeijer, 2018; Grasmeijer et al., 2022). The hydrodynamic and meteorological conditions of the period 2013-2017 were used as input to determine the annual transport rates ono the lower shoreface. From this the mean total, longshore and cross-shore transport was determined and analysed for the cross-shore and longshore zones.

4.2.1 Cross-shore analysis

Figure 8 shows the calculated mean annual transport within the cross-shore zones (colours) and at every grid point of the transport model output (vectors). The total and longshore

transport show similar patterns (Figure 8, left and middle panel) because the longshore transport dominates the cross-shore transport for the Dutch coast. All the cross-shore zones of the northern section accommodate large transport rates compared to the southern section of the coast. The mean longshore transport shows this pattern as well with nearly equal values. The cross-shore transport showed a landward gradient (Figure 8, right panel). Both the vectors and the mean cross-shore transport values in the zones increase towards the boundary at 10 m water depth. The mean transport is onshore for each of the zones. In the northmost part of the coast, north of the narrow section of the shoreface, transport directions are divergent. This is possibly the result diverging currents and hence transport around Hondsbosche Duinen mega nourishment project (e.g. Schuiling, 2019) visible in Figure 7. The increasing cross-shore transport towards the shore (transport gradient) could potentially result in erosion such as observed in Figure 5. The gradient is larger for the northern section, also explaining why the erosion is stronger for that section (Figure 5)

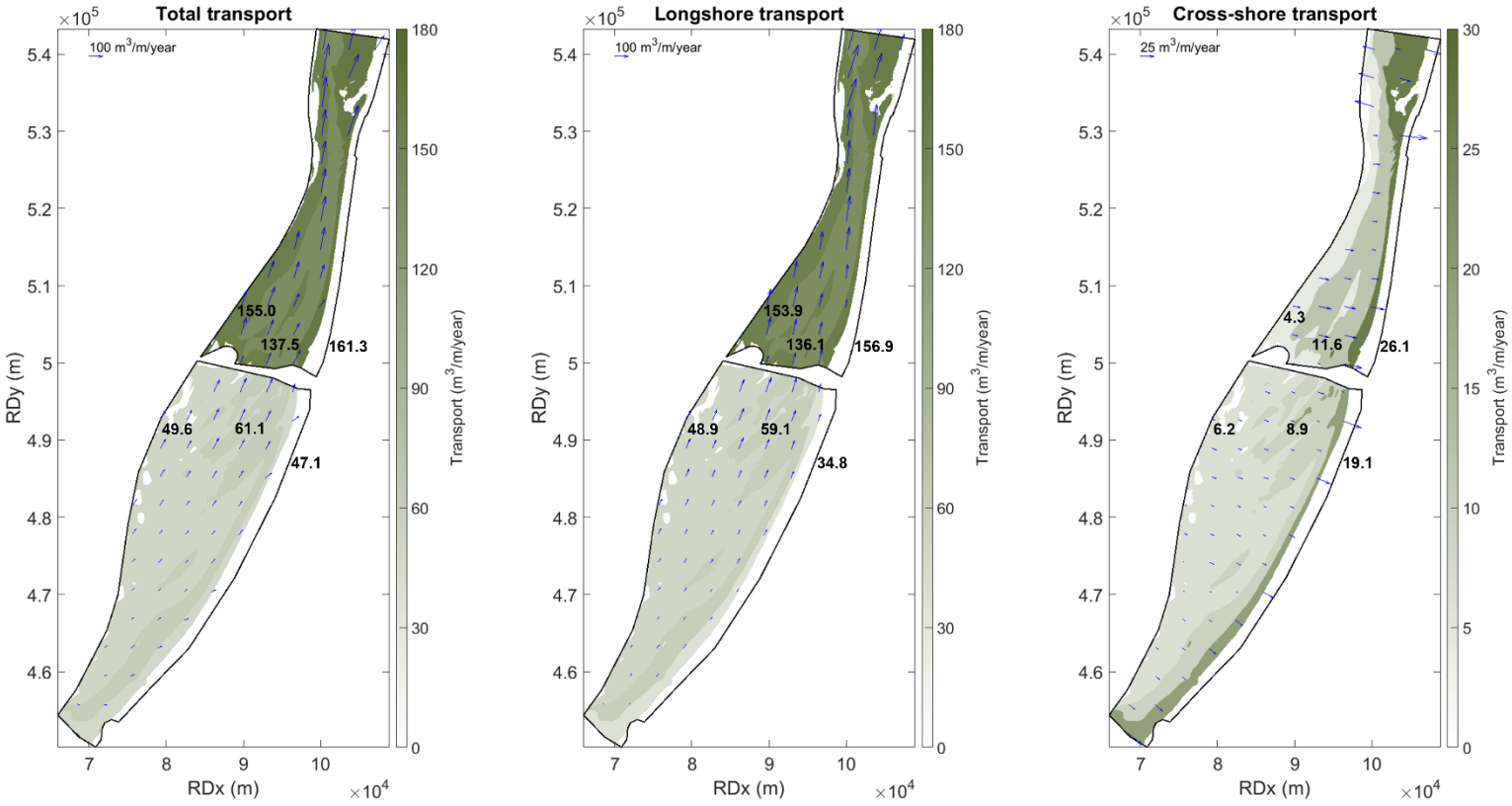

Figure 8: Total (left), longshore (middle) and cross-shore (right) transport for the cross-shore zone.

4.2.2 Longshore analysis

A similar analysis was performed, but with the coast divided into longshore zones. Figure 9 shows the calculated mean total, longshore and cross-shore transport in the longshore zones.

The vectors are the same as described above for the cross-shore zones in Figure 8. Comparable to the analysis for the cross-shore zones, the total and longshore transport values and patterns are comparable since the total transport is dominated by longshore transport. The larger mean transports between the cross-shore zones in northern and southern section of the coast as shown in Figure 8 are now more clearly visible as a longshore gradient in total and longshore transport for the entire Holland coast (Figure 9, left and middle panel). The total and longshore transport increases from small values in the south to large values in the north. The mean transport in the longshore zones increases with a factor over seven from S_{south} towards N_{north}.

The mean cross-shore shows a much different distribution compared to the total and longshore transport (Figure 9, right panel). The mean cross-shore transport is overall onshore-directed, whereas locally it is offshore-directed at some grid points. The mean cross-shore transport is very small within N_{north} with a value of only 0.8 m^3/m/year. The transport vectors show opposing transport directions. The larges mean transports occur in N_{south} and S_{south}.

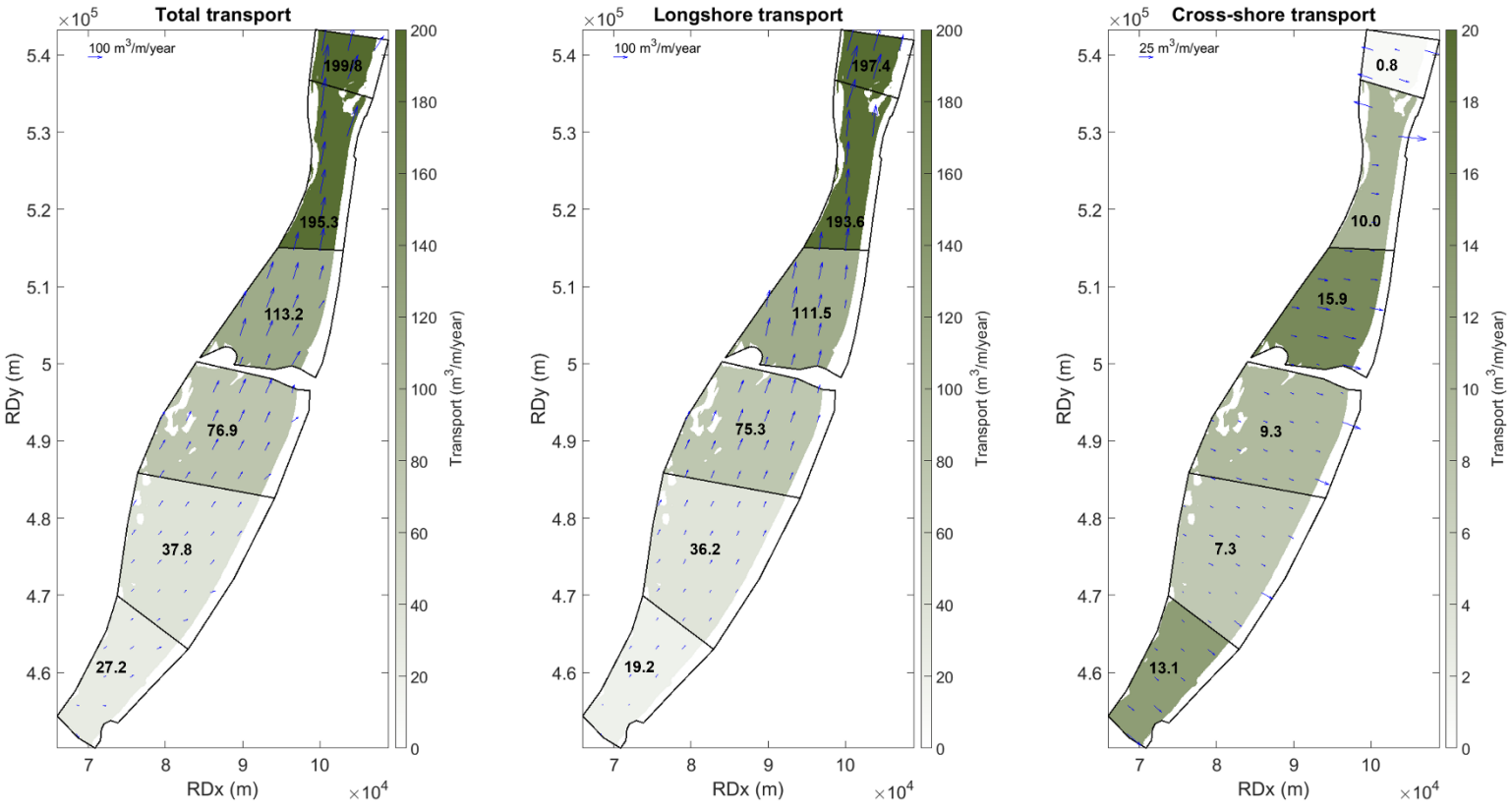

Figure 9: Total (left), longshore (middle) and cross-shore (right) transport for the longshore zones.

4.3 Transport-based sediment volume changes

The change in sediment volume per longshore zone is determined by summing up the integrated sediment transport along the lateral and seaward boundaries. The exchange across

the -10 m NAP contour is excluded because the transport is uncertain in shallow water (Grasmeijer et al., 2022). The results are shown in Figure 10. The black arrows depict the longshore transport along the points of the transects, the coloured arrows represent the mean direction and magnitude of the transport per transect (excluding -10 to 0 m water depth). The numbers in the left panel are the volume changes for the longshore zones in x10^5 m^3/yr. The numbers in the middle and right panel show the volume exchanges across the boundaries in the same units. The transport across the lateral boundaries of the zones increases towards the north similar to Figure 9 in the left panel. At the transect S_{south} transport is primarily directed along the boundary, possibly because the density-driven currents are most strongest in that region close to the Rhine-Meuse river mouths (de Boer, 2009). So, the sediment input from the south is small. At the boundary between zones N_{north} and N_{centre}, the transport vectors show the increase in transport due to flow convergence around the mega nourishment at the Hondsbosche Duinen. The sediment exchanges across the lateral boundaries of the longshore zones depend not only on the transport rates but the length of the boundaries is important as

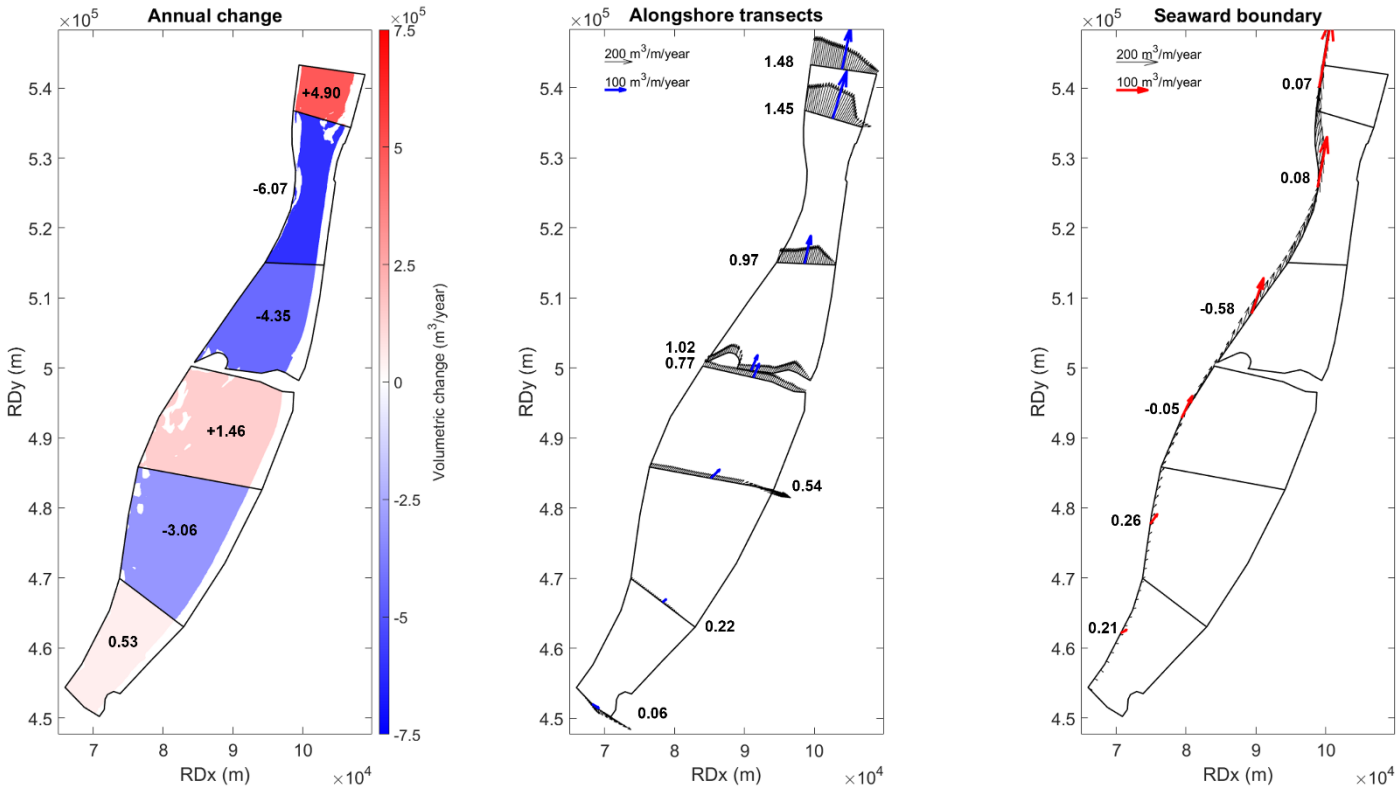

Figure 10: Volumetric changes in sediment in 10^5 m^3/yr based on longshore and cross-shore sediment exchanges. Exchanges with the upper shoreface are not included due to uncertainties in the transport. The middle panel shows the transport directions and rates (vectors) and sediment volume exchange in 10^5 m^3/yr (numbers) across the longshore transects. The right panel shows the transport directions and rates (vectors) and sediment volume exchange in 10^5 m^3/yr (numbers) across the seaward boundary at -20 m NAP. The black vectors are the transport directions and rates along each point of the transects and the coloured arrows represent the mean transport direction and rate for each transect.

well. The curvature in the seaward boundary at -20 m NAP is the result of the variable width of the shoreface of the Holland coast. The curvature results in transport directions obliquely and parallel to the boundary dependant on the location. This results in sediment import where

the shoreface widens and export where the shoreface narrows towards the north. Consequently, sediment exchanges across the seaward boundary sometimes exceed the longshore exchanges.

4.4 Comparison of bathymetry- and transport-based sediment volume change

The change in sediment volume in the longshore zones due to the transport (V_q) was compared with bathymetry-based changes in sediment volumes (V_{bat}). The results are shown in Figure 11. The differences between them were also calculated (V_{diff}). The changes did not match at all. The comparison shows that the changes trends in erosion/accumulation are opposite for all zones except for N_{centre}. The root-mean-square of the difference in volume change is 6.76 x 10^5 m^3/yr which is in most cases larger than the change in sediment volumes determined from the bathymetry and transport. The smallest difference is 1.57 x 10^5 m^3/yr and the largest difference is 1.06 x 10^6 m^3/yr. The large differences suggest either uncertainty in the used data or that sediment exchange with the upper shoreface is important for the observed volume changes.

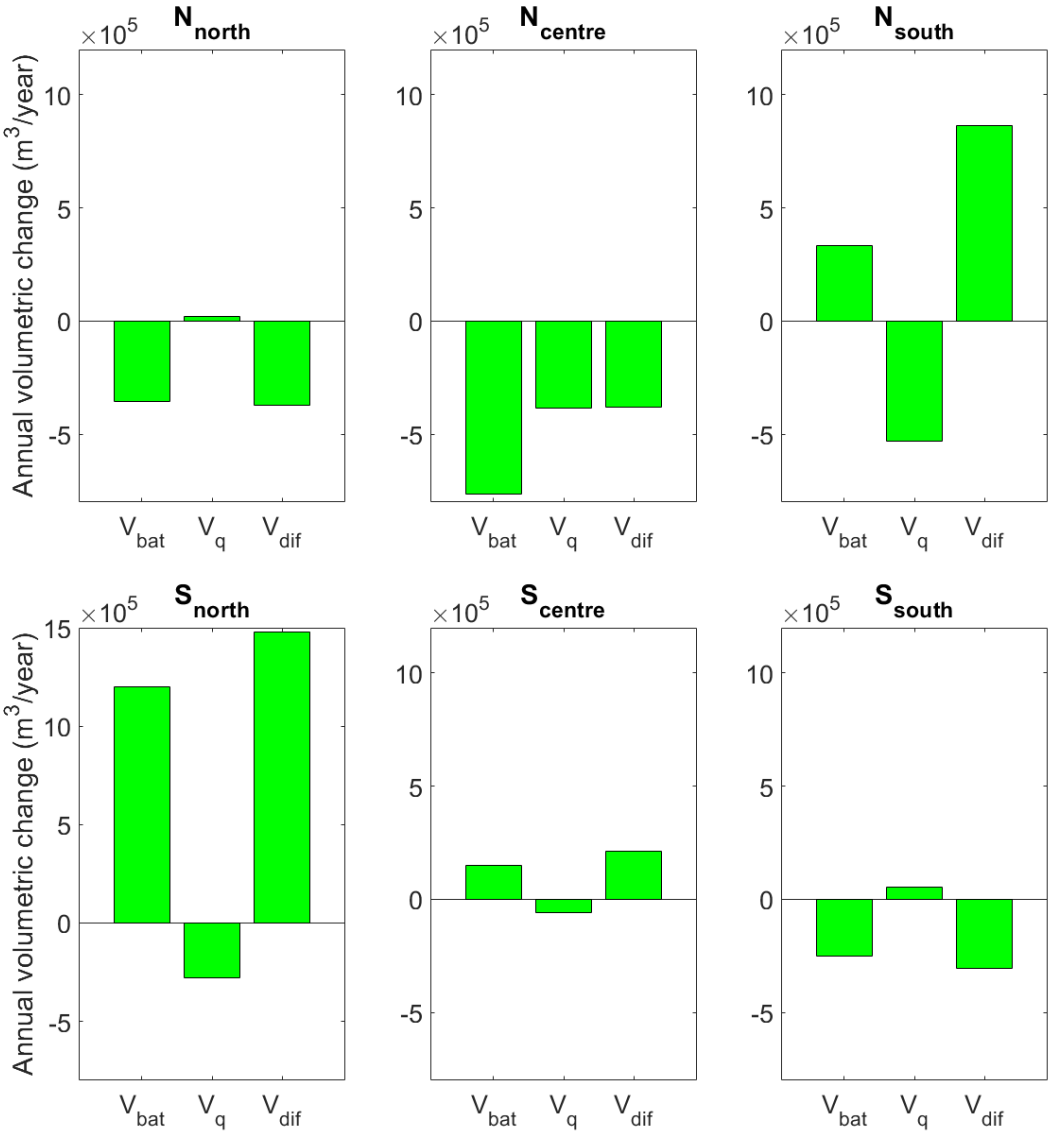

Figure 11: The annual volumetric change based on bathymetric measurements (V_{bat}) and longshore transport across the transects (V_q) for each of the longshore zones. The difference between them is plotted as well as $V_{dif} = V_{bat} - V_q$.

4.5 Key results

The measured mean bed level changes and modelled annual sediment transport rates were studied to quantify the lower shoreface evolution and to point out the responsible sediment exchanges. Here the key results are pointed out:

- The cross-shore zones showed that the lower shoreface is flattening due to relatively large erosion of the shallow part of the lower shoreface compared to small erosion for Noord-Holland and accumulation for Zuid-Holland on the deep part of the lower

shoreface. This is consistent with the findings of Spadon (2000) and the observed lower shoreface deepening by Hinton & Nichols (2007) only holds for Noord-Holland.

- The longshore zones showed that the shoreface can be divided into an eroding norther part, an accreting central part and a relatively stable southern part.
- The mean (Figure 5 and Figure 6) are very small and in the order of centimetres. This also holds for the majority of local (Figure 7) bed level changes. The question arises whether the changes are significant. This point requires further discussion.
- A longshore gradient was present in the modelled longshore and total annual sediment transport due to increasing tidal asymmetry in favour of flood (Grasmeijer et al., 2022).. A cross-shore gradient in onshore-directed cross-shore transport was also found in the modelling results, likely due to increased wave impact.
    - This cross-shore gradient could be an explanation for the flattening of the lower shoreface.
    - Based on the longshore gradient it would be expected to show erosion of the entire shoreface, but this is not the case according to the mean bed level changes in the longshore zones.
    - The longshore transport was the largest near the Hondbosche Duinen mega nourishment, probably due to flow convergence.
- The sediment exchanges based on the modelled transport data depended on the variation in transport and on the shoreface width. The shoreface width modulated the length of lateral boundaries of the zones and resulted in seaward boundary that is oblique to the total transport direction most of the time (meaning import or export of sediment)
- The bathymetry- and transport-based changes in sediment volumes did not match at all and showed opposing trends in accumulatio and erosion. This suggests either that the data is insignificant or that other transport processes govern the bathymetric changes such as transport across the -10 m NAP boundary.

5. Discussion

5.1 Vaklodingen data

5.1.1 Interpolation errors of measured bathymetry

The measured bathymetry is interpolated from transects spaced every kilometre longshore to a 20m x 20 m grid using DIGIPOL. Detailed bed topography is therefore not captured in the grid cells. Longshore oriented and very large features such as bars and shoreface-connected ridges are therefore well captured in Vaklodingen data. Features that are partly oriented cross-shore and small-scale features such as tidal dunes and sandwaves are less well captured in the Vaklodingen data. According to (Perluka et al., 2006), the accuracy after processing the data is 40 cm for the Wadden Sea and Western Scheldt, including the effect of measuring errors to the interpolated bathymetry. This would pose a problem for our study, as the shoreface Dutch shoreface is covered with migrating tidally-induced sand waves, especially at larger water depths (e.g. Van Dijk & Kleinhans, 2005; Vermaas et al., 2015). The interpolation could result in significant under- or overestimation (bias) of the sediment volumes. However, the problem is scale dependent. The bias was found to converge to 0 when using Vaklodingen in polygons larger than 60 km^2, according to Erik van Onselen (Deltares). This information was part of a study that will not be published.

5.1.2 Systematic errors

The outlier that was removed from the study was clearly visible with the naked eye (see Appendix A). This was probably due to a systematic error (Wiegman et al., 2005; Wiegmann et al., 2002). Checking the data for smaller systematic errors (biases) was beyond the time scope of this study. These smaller errors may be larger than the observed bathymetric changes, which would make the measured bathymetric changes uncertain. On the one hand, since results show lower shoreface flattening and deepening consistent with other studies, it is assumed that the trends are at least captured in the data of this study. On the other hand, these biases might be explanatory for the differences observed in the bathymetry- and transport-based sediment volumes. The effect of these biases requires more attention. Moreover, studying the changes over larger periods is an option to make sure that the observed bathymetric changes really happened as they will exceed the biases.

5.1.3 Implications

On the basis of this discussion on Vaklodingen data, the following is suggested to be the case for usage of Vaklodingen at the Holland coast:

- **Usage of the Vaklodingen data on large spatial scales is preferable** – this results in stochastic errors to be cancelled out. Moreover, interpolation biases due to detailed bathymetry (sand waves/dunes/megaripples) are nearly not present at large scales (10 – 100 km).
- **Usage of Vaklodingen data on large temporal scales is preferable** – in this way, bathymetric changes exceed the measuring and interpolation inaccuracies and systematic errors, causing trends to be more obvious and certain.

The first point was implemented in this study. However, the effect of small biases over large areas and consequential errors remains uncertain. Our results should therefore be analysed and interpreted carefully.

5.2 Sediment dynamics on the lower shoreface

5.2.1 Cross-shore sediment exchange across the -10 m NAP boundary

Due to uncertainty in the modelling results of Grasmeijer et al. (2022), the sediment exchange with the upper shoreface was excluded. However, the transport rates generally increase towards the shore (e.g. Patterson & Nielsen, 2016). The sediment exchange of sediment across the -10 m NAP boundary is likely to have a large effect on the volume change within the longshore zones of Figure 10. The modelled annual transport is onshore, so it is an output of sediment for the lower shoreface. An estimation of the cross-shore transport based on the length of the coast and the mean annual transport for the cross-shore zones between -14 and -10 m NAP suggest an exchange of at least 1.0×10^6 m^3/yr. However, Van Rijn (1997) showed that 4.9×10^5 m^3/year was supplied annually from the zone seaward of -8 m NAP to the upper shoreface. An exchange with the upper shoreface would result in a smaller difference for the bathymetry- and transport-based sediment volumes for N_{north}, N_{centre} and S_{south} but would have an opposite effect for the other zones.

5.2.2 Return currents effects

Return currents are not included in the modelled transport data. This has two effects for the observed volumetric changes due to the longshore transport. Firstly, the return currents result in increased offshore or decreased onshore transport across the seaward boundary at -20 m NAP. However, the currents are primarily present in shallow water depths and during high wave energy events. Thus, the offshore transport at -20 m NAP will not be as large compared to other currents (density, wind, tidal). Though, the annual transports may be 11-20% smaller at across the -20 m NAP boundary the currents are included (Grasmeijer et al., 2022). Secondly, it counteracts the observed onshore transport across the -10 m NAP boundary, causing smaller net onshore transports or even net offshore transport. The importance of return currents has been marked previously in literature as an important driver of sediment dynamics, however primarily on the upper shoreface (e.g. Knook, 2013; Mariño-Tapia et al., 2007). Return currents at -10 m NAP will exceed those at -20 m NAP. Therefore, the net effect is that return currents will reduce the amount of sediment that is lost to onshore transport from the lower towards the upper shoreface. This means that the transport-based volumetric changes will be higher or less negative than we calculated. Also, the cross-shore transport gradient in Figure 8 will be smaller, thus losses to the upper shoreface will be smaller as well. Return currents are slope-dependant (e.g Knook, 2013) and might show variations along the shoreface. The effect of including return currents would thus be alongshore variable.

5.2.3 Vicinity of tidal inlet systems

Another factor that might explain the deviation between the bathymetric measurements and the longshore transport-based method is the presence of the tidal inlet to the north and south of the coast as well. The 3D DCSM-FM model has a resolution of 840 by 930 m near the shore. Near tidal inlets such as in N_{north} and S_{south}, the resolution is most certainly too coarse to accurately model the flow the complex situation at tidal inlets with respect to flow patterns and the bathymetry of ebb-tidal morphologies (e.g. Nederhoff, 2019). Therefore, the transport model output used is uncertain near the inlets. This should cause a large deviation in the determined volumetric change.

6. Conclusions

The aim of the study is to quantify the large-scale bed level changes, to find the responsible sediment exchanges and to validate the transport model results of Grasmeijer et al. (2022). Bathymetric changes based on Vaklodingen between 2019-2017 and transport data between 2013-2017 from Grasmeijer et al. (2022) are combined to study the shoreface of the Dutch Holland coast. The lower shoreface shows flattening due to larger net erosion of the shallow part compared to smaller net erosion (Noord-Holland) or net accumulation (Zuid-Holland) in the deeper part. The northern part of the lower shoreface shows net erosion, the middle part net accumulation and the southern part is relatively stable (mean result over the entire depth). The modelled transport data shows an increasing total and longshore transport towards the north due to increasing tidal flood dominance (Grasmeijer et al., 2022). The cross-shore transport is generally onshore and increased towards smaller water depths due to increased wave effects. The modelled transports results in longshore and cross-shore exchanges. These are dependent on the transport magnitude, the shoreface width and the vicinity of mega nourishment. The shoreface width modulates the length of the lateral boundaries and results in a curving seaward boundary so that transport is oblique to this boundary most of the time. This results in alongshore variable inputs and outputs for the different zones. Additionally, sediment volume changes are determined based on the measured bathymetry and on the modelled transport. The results show almost no resemblance. This is for unknown reasons. Possible explanations are inaccuracies of the bathymetric data, the excluded sediment exchange with the upper shoreface and the excluded effect of undertow in the transport model results. The study is designed to overcome the uncertainties that come with Vaklodingen usage, however, the results must be taken in carefully. It is suggested that uncertainties in Vaklodingen data require more attention. Studying the changes over a longer period so that they are larger is also a solution to the uncertainties Nevertheless, the combination of the bathymetry and transport data of this study provides useful information for coastal management.

References

Aagaard, T. (2011). Sediment transfer from beach to shoreface: The sediment budget of an accreting beach on the Danish North Sea Coast. *Geomorphology*, *135*(1–2), 143–157. https://doi.org/10.1016/j.geomorph.2011.08.012

Aagaard, T. (2014). Sediment supply to beaches: Cross-shore sand transport on the lower shoreface. *Journal of Geophysical Research: Earth Surface*, *119*, 913–926. https://doi.org/10.1002/2013JF002871.Received

Aagaard, T., & Greenwood, B. (1994). Suspended sediment transport and the role of infragravity waves in a barred surf zone. *Marine Geology*, *118*, 23–48.

Aagaard, T., & Kroon, A. (2007). MESOSCALE BEHAVIOUR OF LONGSHORE BARS – NET ONSHORE OR NET OFFSHORE MIGRATION. *Proceedings Coastal Sediments*, *7*, 2124–2136.

Anthony, E. J. (2013). Storms, shoreface morphodynamics, sand supply, and the accretion and erosion of coastal dune barriers in the southern North Sea. *Geomorphology*, *199*, 8–21. https://doi.org/10.1016/j.geomorph.2012.06.007

Anthony, E. J., & Aagaard, T. (2020). The lower shoreface: Morphodynamics and sediment connectivity with the upper shoreface and beach. *Earth-Science Reviews*, *210*(August). https://doi.org/10.1016/j.earscirev.2020.103334

Backstrom, J. T., Jackson, D. W. T., & Cooper, J. A. G. (2009). Shoreface morphodynamics of a high-energy, steep and geologically constrained shoreline segment in Northern Ireland. *Marine Geology*, *257*(1–4), 94–106. https://doi.org/10.1016/j.margeo.2008.11.002

Baldock, T. E., Manoonvoravong, P., & Pham, K. S. (2010). Sediment transport and beach morphodynamics induced by free long waves, bound long waves and wave groups. *Coastal Engineering*, *57*, 898–916. https://doi.org/10.1016/j.coastaleng.2010.05.006

Battjes, J. A., Bakkenes, H. J., Janssen, T. T., & Van Dongeren, A. R. (2004). Shoaling of subharmonic gravity waves. *J. Geophys. Res*, *109*, 2009. https://doi.org/10.1029/2003JC001863

Bertin, X., de Bakker, A., van Dongeren, A., Coco, G., André, G., Ardhuin, F., … Tissier, M. (2018). Infragravity waves: From driving mechanisms to impacts. *Earth-Science Reviews*, *177*, 774–799. https://doi.org/10.1016/j.earscirev.2018.01.002

Brand, E., Ramaekers, G., & Lodder, Q. (2022). Dutch experience with sand nourishments for dynamic coastline conservation – An operational overview. *Ocean and Coastal Management*, *217*(March 2021), 106008. https://doi.org/10.1016/j.ocecoaman.2021.106008

Brunel, C., Certain, R., Sabatier, F., Robin, N., Barusseau, J. P., Aleman, N., & Raynal, O. (2014). 20th century sediment budget trends on the Western Gulf of Lions shoreface (France): An application of an integrated method for the study of sediment coastal reservoirs. *Geomorphology*, *204*, 625–637. https://doi.org/10.1016/j.geomorph.2013.09.009

Castelle, B., Marieu, V., Bujan, S., Splinter, K. D., Robinet, A., Sénéchal, N., & Ferreira, S. (2015). Impact of the winter 2013-2014 series of severe Western Europe storms on a double-barred sandy coast: Beach and dune erosion and megacusp embayments. *Geomorphology*, *238*, 135–148. https://doi.org/10.1016/j.geomorph.2015.03.006

da Motta, L. M., Toldo, E. E., de Almeida, L. E. de S. B., & Nunes, J. C. (2015). Sandy sediment budget of the midcoast of Rio Grande do Sul, Brazil. *Journal of Marine Research*, *73*(3–4), 49–69. https://doi.org/10.1357/002224015815848839

De Bakker, A. T. M., Herbers, T. H. C., Smit, P. B., Tissier, M. F. S., & Ruessink, B. G. (2015). Nonlinear Infragravity-Wave Interactions on a Gently Sloping Laboratory Beach. *Journal of Physical Oceanography*, 589–605. https://doi.org/10.1175/JPO-D-14-0186.1

de Boer, G. J. (2009). *On the interaction between tides and stratification in the Rhine Region of Freshwater Influence*. Retrieved from http://www.narcis.nl/publication/RecordID/oai:tudelft.nl:uuid:c5c07865-be69-4db2-91e6-f675411a4136%0Ahttp://repository.tudelft.nl/view/ir/uuid:c5c07865-be69-4db2-91e6-f675411a4136/

de Winter, R. C., Gongriep, F., & Ruessink, B. G. (2015). Observations and modeling of alongshore variability in dune erosion at Egmond aan Zee, the Netherlands. *Coastal Engineering*, *99*, 167–175. https://doi.org/10.1016/j.coastaleng.2015.02.005

Dronkers, J. (1986). Tidal asymmetry and estuarine morphology. *Netherlands Journal of Sea Research*, *20*(2–3), 117–131. https://doi.org/10.1016/0077-7579(86)90036-0

Elias, E. P. L., & Van Der Spek, A. J. F. (2017). Dynamic preservation of Texel Inlet, the Netherlands: Understanding the interaction of an ebb-tidal delta with its adjacent coast. *Geologie En Mijnbouw/Netherlands Journal of Geosciences*, *96*(4), 293–317. https://doi.org/10.1017/njg.2017.34

Ellen Quataert, Stephanie IJff, & Marc Hijma. (2021). *Beheerbibliotheek Kust Delfland*.

Giardino, A., van der Werf, J., & van Ormondt, M. (2010). *Simulating Coastal Morphodynamics with Delft3D: case study Egmond aan Zee*. Retrieved from http://publications.deltares.nl/1200635_005.pdf

Grasmeijer, B. (2018). *Method for Calculating Sediment Transport on the Dutch Lower Shoreface*. 25.

Grasmeijer, B., Huisman, B., Luijendijk, A., Schrijvershof, R., van der Werf, J., Zijl, F., … de Vries, W. (2022). Modelling of annual sand transports at the Dutch lower shoreface. *Ocean & Coastal Management*, *217*(December 2021), 105984. https://doi.org/10.1016/j.ocecoaman.2021.105984

Grunnet, N. M., Walstra, D. J. R., & Ruessink, B. G. (2004). Process-based modelling of a shoreface nourishment. *Coastal Engineering*, *51*(7), 581–607. https://doi.org/10.1016/j.coastaleng.2004.07.016

Hamon-Kerivel, K., Cooper, A., Jackson, D., Sedrati, M., & Guisado Pintado, E. (2020). Shoreface mesoscale morphodynamics: A review. *Earth-Science Reviews*, *209*(February). https://doi.org/10.1016/j.earscirev.2020.103330

Hapke, C. J., Lentz, E. E., Gayes, P. T., McCoy, C. A., Hehre, R., Schwab, W. C., & Williams, S. J. (2010). A review of sediment budget imbalances along fire Island, New York: Can nearshore geologic framework and patterns of shoreline change explain the deficit? *Journal of Coastal Research*, *26*(3), 510–522. https://doi.org/10.2112/08-1140.1

Hassan, W. N., & Ribberink, J. S. (2005). Transport processes of uniform and mixed sands in oscillatory sheet flow. *Coastal Engineering*, *52*(9), 745–770. https://doi.org/10.1016/j.coastaleng.2005.06.002

Héquette, A., Hemdane, Y., & Anthony, E. J. (2008). Sediment transport under wave and current combined flows on a tide-dominated shoreface, northern coast of France. *Marine Geology*, *249*(3–4), 226–242. https://doi.org/10.1016/j.margeo.2007.12.003

Hinton, C. L., & Nicholls, R. J. (2007). Shoreface morphodynamics along the Holland coast. *Geological Society Special Publication*, *274*, 93–101. https://doi.org/10.1144/GSL.SP.2007.274.01.10

Hoekstra, P., Houwman, K. T., Kroon, A., Ruessink, B. G., Roelvink, J. A., & Spanhoff, R. (1997). Morphological development of the Terschelling shoreface nourishment in response to hydrodynamic and sediment transport processes. *Proceedings of the Coastal Engineering Conference*, *3*, 2897–2910. https://doi.org/10.1061/9780784402429.224

Holman, R. A., Huntley, D. A., & Bowen, A. J. (1978). INFRAGRAVITY WAVES IN STORM CONDITIONS. *Coastal Engineering Proceedings*, *1*(16). https://doi.org/10.9753/ICCE.V16.%P

Hsu, T. J., Elgar, S., & Guza, R. T. (2006). Wave-induced sediment transport and onshore sandbar migration. *Coastal Engineering*, *53*(10), 817–824. https://doi.org/10.1016/j.coastaleng.2006.04.003

Huisman, B. J.A., Ruessink, B. G., de Schipper, M. A., Luijendijk, A. P., & Stive, M. J. F. (2018). Modelling of bed sediment composition changes at the lower shoreface of the Sand Motor. *Coastal Engineering*, *132*(November 2017), 33–49. https://doi.org/10.1016/j.coastaleng.2017.11.007

Huisman, Bastiaan J.A., Walstra, D. J. R., Radermacher, M., de Schipper, M. A., & Ruessink, B. G. (2019). Observations and modelling of shoreface nourishment behaviour. *Journal of Marine Science and Engineering*, *7*(3). https://doi.org/10.3390/jmse7030059

King, E. V., Conley, D. C., Masselink, G., Leonardi, N., McCarroll, R. J., & Scott, T. (2019). The Impact of Waves and Tides on Residual Sand Transport on a Sediment-Poor, Energetic, and Macrotidal Continental Shelf. *Journal of Geophysical Research: Oceans*, *124*(7), 4974–5002. https://doi.org/10.1029/2018JC014861

Kleinhans, M. G., & Grasmeijer, B. T. (2006). Bed load transport on the shoreface by currents and waves. *Coastal Engineering*, *53*(12), 983–996. https://doi.org/10.1016/j.coastaleng.2006.06.009

Knook, P. . (2013). *Sediment transport on various depth contours of the ' Holland Coast ' shoreface*. (January).

Loureiro, C., Ferreira, Ó., & Cooper, J. A. G. (2012). Extreme erosion on high-energy embayed beaches: Influence of megarips and storm grouping. *Geomorphology*, *139–140*, 155–171. https://doi.org/10.1016/j.geomorph.2011.10.013

Mariño-Tapia, I. J., Russell, P. E., O'Hare, T. J., Davidson, M. A., & Huntley, D. A. (2007). Cross-shore sediment transport on natural beaches and its relation to sandbar migration patterns: 1. Field observations and derivation of a transport parameterization. *Journal of Geophysical Research: Oceans*, *112*(3), 1–15.

https://doi.org/10.1029/2005JC002893

Navas, F., Cooper, A., Malvares, G. C., & Jackson, D. W. T. (2001). Theoretical Approach to the Investigation of Ridge and Runnel Topography of a Macrotidal Beach: Dundrum Bay, Northern Ireland. *Journal of Coastal Research*, *12*.

Nederhoff, C. M., Schrijvershof, R., Tonnon, P. K., & van der Werf, J. J. (2019). *The Coastal Genesis II Terschelling - Ameland inlet (CGII-TA) model*.

Nielsen, P. (2006). Sheet flow sediment transport under waves with acceleration skewness and boundary layer streaming. *Coastal Engineering*, *53*(9), 749–758. https://doi.org/10.1016/j.coastaleng.2006.03.006

Ortiz, A. C., & Ashton, A. D. (2016). Exploring shoreface dynamics and a mechanististic explanation for a morphodynamic depth of closure. *Journal of Geophysical Research: Earth Surface*, 300–316. https://doi.org/10.1002/2013JF002871.Received

Patterson, D. C., & Nielsen, P. (2016). Depth, bed slope and wave climate dependence of long term average sand transport across the lower shoreface. *Coastal Engineering*, *117*, 113–125. https://doi.org/10.1016/j.coastaleng.2016.07.007

Perluka, R., Wiegmann, E. B., Jordans, R. W. L., & Swart, L. M. T. (2006). *Opnametechnieken Waddenzee opq Opnametechnieken Waddenzee*.

Reniers, A. J. H. M., Macmahan, J. H., Thornton, E. B., & Stanton, T. P. (2006). Modelling infragravity motions on a rip-channel beach. *Coastal Engineering*, *53*, 209–222. https://doi.org/10.1016/j.coastaleng.2005.10.010

Rijkswaterstaat. (2020). *Kustgenese 2.0: kennis voor een veilige kust*.

Roelvink, D., Reniers, A., Van Dongeren, A., Van Thiel De Vries, J., Mccall, R., & Lescinski, J. (2009). Modelling storm impacts on beaches, dunes and barrier islands. *Coastal Engineering*, *56*, 1133–1152. https://doi.org/10.1016/j.coastaleng.2009.08.006

Ruessink, B. G., Houwman, K. T., & Hoekstra, P. (1998). Medium-term frequency distributions of cross-shore suspended sediment transport rates in water depths of 3 to 9 m. *Marine Geology*, *152*, 295–324. https://doi.org/10.1016/S0378-3839(99)00023-X

Ruessink, B. G., Miles, J. R., Feddersen, F.Guza, R. T., & Elgar, S. (2001). Modeling the alongshore current on barred beaches. *Journal of Geophysical Research*, *106*(22), 451–463.

Ruessink, B. G., Ramaekers, G., & Van Rijn, L. C. (2012). On the parameterization of the free-stream non-linear wave orbital motion in nearshore morphodynamic models. *Coastal Engineering*, *65*, 56–63. https://doi.org/10.1016/j.coastaleng.2012.03.006

Schuiling, T. H. (2019). *Suppletiebehoefte van de Nederlandse kust*. Universiteit Twente.

Spadon, Y. J. A. (2000). *Versteiling van de Hollandse kust nader bekeken*. TU Delft.

Spek, A. van der, Werf, J. van der, Grasmeijer, B., Vreugdenhil, H., Oeveren-Theeuwes, C. van, & Nolte, A. (2020). *Technisch Advies Mogelijkheid voor een Alternatieve Zeewaartse Grens van het Kustfundament*.

Stive, M. J. F., & de Vriend, H. J. (1995). Modelling shoreface profile evolution. *Marine Geology*, *126*(1–4), 235–248. https://doi.org/10.1016/0025-3227(95)00080-I

Thornton, E. B., MacMahan, J., & Sallenger, A. H. (2007). Rip currents, mega-cusps, and eroding dunes. *Marine Geology*, *240*(1–4), 151–167. https://doi.org/10.1016/j.margeo.2007.02.018

Van de Meene, J. W. H., & Van Rijn, L. C. (2000). The shoreface-connected ridges along the central Dutch coast - Part 1: Field observations. *Continental Shelf Research*, *20*(17), 2295–2323. https://doi.org/10.1016/S0278-4343(00)00048-0

Van der Werf, J. J., Grasmeijer, B., Hendriks, E., Van der Spek, A. J. F., & Vermaas, T. (2017). *Literature study Dutch lower shoreface*. 97.

Van Dijk, T. A. G. P., & Kleinhans, M. G. (2005). Processes controlling the dynamics of compound sand waves in the North Sea, Netherlands. *Journal of Geophysical Research: Earth Surface*, *110*(4). https://doi.org/10.1029/2004JF000173

van Rijn, L. C. (2007). Unified View of Sediment Transport by Currents and Waves. III: Graded Beds. *Journal of Hydraulic Engineering*, *133*(7), 761–775. https://doi.org/10.1061/(asce)0733-9429(2007)133:7(761)

Van Rijn, L. C. (1997). Sediment transport and budget of the central coastal zone of Holland. *Coastal Engineering*, *32*(1), 61–90. https://doi.org/10.1016/S0378-3839(97)00021-5

van Rijn, L. C., Walstra, D.-J. R., & van Ormondt, M. (2007). Unified View of Sediment Transport by Currents and Waves. IV: Application of Morphodynamic Model. *Journal of Hydraulic Engineering*, *133*(7), 776–793. https://doi.org/10.1061/(asce)0733-9429(2007)133:7(776)

Vermaas, T., van Dijk, T., & Hijma, M. (2015). *Bodemdynamiek van de diepe onderwateroever met oog op de -20 m NAP lijn*.

Verschure, J. W. . (2014). *The importance of infragravity waves in the cross-shore sediment transport in the surf zone of a barred intertidal beach* (Utrecht University). Retrieved from http://dspace.library.uu.nl:8080/handle/1874/292943

Vidal-Ruiz, J. A., & Ruiz de Alegría-Arzaburu, A. (2019). Variability of sandbar morphometrics over three seasonal cycles on a single-barred beach. *Geomorphology*, *333*, 61–72. https://doi.org/10.1016/j.geomorph.2019.02.034

Walburg, L. (2005). *Zandvolumes in het Nederlandse kustsysteem*. (RIKZ/KW/2005.133w).

Wiegman, N., Perluka, R., Oude Elberink, S., & Vogelzang, J. (2005). *Vaklodingen: de inwintechnieken en hun combinaties. Vergelijking tussen verschillende inwintechnieken en de combinaties ervan*. 47.

Wiegmann, N., Perluka, R., & Boogaard, K. (2002). *Onderzoek naar efficiency verbetering kustlodingen*. (december).

Witteveen, M. (2012). *Cross-shore suspended sediment transport and morphological response on a beach plain during fair weather conditions and during a storm event at The Slufter , Texel Cross-shore suspended sediment transport and morphological response on a beach plain during*. Utrecht University.

Zijl, F., Veenstra, J., & Groenenboom, J. (2018). The 3D Dutch Continental Shelf Model - Flexible Mesh (3D DCSM-FM). In *2018*.

Appendix A

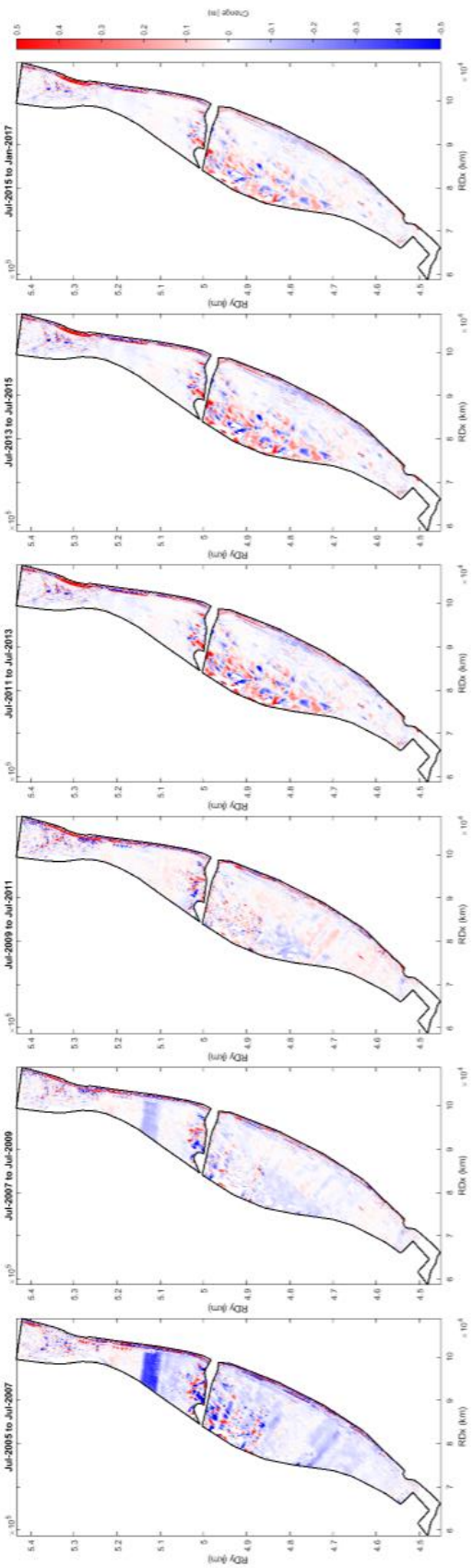

Bathymetric changes between 2005 and 2017 in per two years. 2005-2007 and 2007-2009 shows an rectangular area of strong erosion, probably due a systematic error in the measurements.